A Review of Microwave-assisted Process Intensified Multiphase Reactors

Himanshu Goyal[1*], Tai-Ying Chen[2,3], Weiqi Chen[2,3], and Dionisios G. Vlachos[2,3*]

1. Department of Chemical Engineering, Indian Institute of Technology Madras, Chennai, Tamil Nadu 600036, India
2. Department of Chemical and Biomolecular Engineering, University of Delaware, 150 Academy St., Newark, Delaware 19716, United States
3. Catalysis Center for Energy Innovation and RAPID Manufacturing Institute, 221 Academy St., Newark, DE 19716, United States

*Corresponding authors: Himanshu Goyal (goyal@iitm.ac.in) and Dionisios G. Vlachos (vlachos@udel.edu)

Abstract

Microwaves provide alternative heating and allow process intensification due to their rapid, volumetric, and selective nature. Recognizing the central role of multiphase reactors in chemical industry, a recent surge in employing microwaves is observed. Here, we review the recent experimental and modeling investigations of microwave heating of multiphase reactors with emphasis on chemical engineering applications. We demonstrate that there is accumulated evidence for improved performance via microwave heating and a clear opportunity for further process intensification. In most of the cases, this improved performance stems from a temperature gradient between two phases. We discuss the ongoing debate on the mechanism by which microwaves affect chemical processes exacerbated by the inability of measuring the

temperature distribution in a microwave cavity. We outline recent progress in this direction in monolith reactors and needs for future work. We underscore the lack of detailed modeling and simulation tools even for single-phase systems and emphasize the imperative for multiscale predictive modeling to bridge the experimental-modeling gap. Promising results are shown by a few recently published modeling studies that can predict the experimental measurements in complex multiphase reactors. A combination of experimental and modeling tools can provide a comprehensive picture of the microwave multiphase reactors as well as a means toward scale-up and optimization.

Keywords: microwave heating, multiphase reactors, process intensification, multiscale modeling, selective heating

Contents

1. Introduction
2. Fundamentals of microwave heating
    2.1 Microwave heating mechanisms
    2.2 Temperature measurement during microwave heating
3. Process intensification in microwave multiphase reactors
    3.1 Fluid-fluid systems
        3.1.1 Dispersed systems
        3.1.2 Biphasic systems
    3.2 Fluid-solid systems
        3.2.1 Slurry reactors

3.2.2 Fixed bed reactors

3.2.3 Structured reactors

3.3 Discussion on hot spots and arcing

3.4 Summary of the experimental multiphase reactor studies: reaction selection and scale-up

4. Modeling of microwave heated reactors

4.1 Microwave heating using simplified approaches

4.2 Multiscale modeling

5. Conclusions and outlook

Appendix: Governing equations

1. Introduction

The cost of electricity production from solar and wind has substantially declined in the past decades and continues to decrease [1]. Microwaves, produced from affordable renewable electricity, can help in the chemical industry's electrification by providing an alternative to conventional heating of chemical reactors currently run on fossil fuels. Besides, the rapid, volumetric, and selective nature of microwave heating, it offers a new paradigm in designing chemical reactors with significant potential for process intensification, i.e., achieving a substantial improvement in at least one of the process parameters, such as yield, selectivity, capital or operating cost, and environmental impact.

Historically, microwave heating has been applied commercially in food processing, wood drying, plastic and rubber treating, and curing and preheating ceramics [2]. Application of

microwave heating to chemical engineering processes remains mostly unexplored. In the last decade, research in this direction has gained momentum with several groups exploring the process intensification potential of microwaves in some of the most challenging chemical engineering problems. For example, ammonia production at low pressure [3] and methane and biomass valorization [4, 5]. These recent investigations are promising and pose further research questions.

Most industrial chemical reactors, such as fixed beds, fluidized beds, slurries, and monoliths are multiphase. The selective nature of microwave heating, i.e., preferential heating of a phase or material compared to others, plays a vital role in multiphase reactors. For example, in a silicon carbide monolith, microwaves get converted into heat only in the solid phase and not in the gas present in the monolith channels. Thus, selective heating can create a temperature gradient between different phases, impacting the homogeneous and heterogeneous reactions in the reactor. Such behavior is the most distinguishing characteristic of microwave heating of multiphase reactors and cannot be obtained in conventional heating.

Selective heating can also lead to highly localized heating or hot spot formation [6], sometimes associated with arcing or plasma [7], usually occurring when the electric field gets concentrated in a small gap between microwave absorbers, such as activated carbon and silicon carbide [7, 8]. When the electric field strength becomes higher than the dielectric strength of the continuum phase (~3 MV/m for air) arcing or plasma occurs [9]. Sharp edges and other surface irregularities assist arc formation as free charges accumulate in those regions, increasing the charge density and the resulting electric field [8, 9]. These unique features of microwave heating in multiphase reactors can be useful [10, 11] or detrimental [12]. For example, hot spots can

crystallize the metal nanoparticles dispersed on catalyst support reducing their efficacy [13, 14]; however, hot spots can also enhance the reaction performance by allowing the heterogeneous reactions to occur at a higher temperature [15, 16] or by increasing the product's desorption rate from the catalyst surface [17].

In the past decade, several experimental works have focused on microwave multiphase reactors, such as monoliths [5, 18-22], fixed beds [23-25], and slurry reactors [7, 11, 12, 14-16]. Applications of these investigations include polymerization [26], biomass valorization [27, 28], epoxidation [29, 30], methane non-oxidative coupling [5], and propane dehydrogenation [22]. These recent explorations are encouraging as they demonstrate the potential of microwave heating in achieving process intensification, especially in terms of higher yields and selectivity, and lower processing time. The observed differences between the microwave heating and conventional heating are most often attributed to the thermal effects, i.e., non-uniform temperature distribution or higher solid temperature than the fluid phase. However, only a few works [5, 19, 21] have measured the different phases' temperature with sufficient spatial resolution.

There has been an ongoing debate on how microwaves affect chemical transformations. While most investigators [5, 19-21] support the view that microwaves only have a thermal effect, a few propose that microwave radiation reduces the activation energy of chemical reactions, known as the non-thermal or microwave-specific effect [31-33]. These latter studies are performed in a fixed bed and measured the surface temperature using an infrared pyrometer or local temperature inside the bed using a thermocouple. Thus, the temperature field with sufficient spatial resolution is not available, hindering conclusive evidence. Some of the reported

microwave-specific effects are ultimately related to thermal effects. For example, Bruyn et al. [6] performed numerical simulations to analyze the observed change in the reaction order in a microwave heated reaction system consisting of gas bubbles in a liquid. They showed that the localized microwave heating near the bubble-liquid interface causes a significant increase in the number of bubbles leading to enhanced removal of the gaseous byproducts and changing the observed reaction order. In another system consisting of metal particles in a solvent, microwave heating decelerated the reaction due to arcing, which decomposed the solvent forming a carbonaceous layer on the metal particles resulting in reaction slowing down [34].

Kappe and co-workers [35-38] have worked extensively to disprove the non-thermal effects of microwaves by using silicon carbide vials with the assumption that silicon carbide shields the reaction mixture from microwaves by converting most of the microwaves into heat within the vial. However, significant microwave leakage (~52%) into silicon carbide vials with 3 mm wall thickness has been reported [39]. These contradicting observations do not permit an authoritative claim about the non-thermal effects postulated in the latest literature [3, 32]. Recently developed infrared (IR) thermographic technique by Santamaria and co-workers [5, 19, 21] to measure the gas and solid phases' temperature in monolith reactors brings some clarity to this topic. The technique relies on simultaneous usage of a calibrated IR pyrometer, thermographic camera, and thermocouples. Santamaria and co-workers [5, 19, 21] showed that for various catalytic reactions, the improved reactor performance under microwave radiation could be explained by the temperature gradient between the gas and solid phases. These recent studies point that inaccurate measurements or measurement of a point temperature have led to the suggestion of the microwave radiation's non-thermal effect on chemical transformations.

Accurate measurement and prediction of temperature distribution with sufficient spatial resolution within a reactor remain a critical challenge in understanding how microwaves affect a chemical process.

Apart from the challenge of temperature measurement, other issues also hamper the development of microwave heating-based technologies. For example, difficulty in microwave cavity design due to the sensitive nature of the standing wave pattern of the electric and magnetic fields and ineffective heating of the reactor during scale-up as the penetration depth becomes smaller than the reactor size. During scale-up only an outer layer of the reactor gets heated, leaving a relatively colder inner region. Widespread application of microwave heating in chemical industries would require managing these challenges.

Progress in computational resources and user-friendly multiphysics commercial software could rectify some of the present experimental limitations by providing the precise temperature and electromagnetic field distribution in a microwave cavity and reactor. However, progress in computational modeling is lagging compared to the advances in experiments. Modeling of microwave multiphase reactors is challenging due to their multiphase (e.g., gas-solid and gas-liquid), multiphysics (e.g., electromagnetism, transport processes, and chemical reactions), and multiscale (e.g., length scale varying from a single catalyst particle to the microwave cavity) nature. Only a few simulation studies exist that perform an assessment against experimental measurements even in lab-scale reactors [40-44]. Most of these studies have been performed for single-phase systems, such as microwave heating of liquids in a glass vial [40, 41, 44]. For multiphase systems, several simplifications are made to handle the complexity and reduce the computational cost. For example, simulating an experimental fixed bed with uniformly arranged

large particles [24] and assuming the biphasic solid hydride [45] and zeolite fixed bed [46] to be a continuum using the experimentally measured effective permittivity of the sample. These simplifications could add large uncertainties in the model predictions, making their usage unreliable for reactor design. Currently, predictive simulation tools for microwave heating of multiphase systems are scarce. Only a few simulation studies exist that consider the exact experimental geometry in the computational setup [43]. Development of robust modeling and simulation tools is imperative to understand and assist in the design of multiphase microwave reactors. A primary objective for such modeling tools should be the accurate prediction of the three-dimensional temperature field within microwave heated reactors, which at present cannot be measured experimentally.

Several reviews are available about microwave reactor design [47], energy efficiency of microwave heating [48], scaleup of microwave reactors [49], and microwave heating for different applications, such as catalysis [50], food industry [51], organic chemistry [35], biomass thermochemical conversion [4, 52-56], nanoparticles synthesis [57], and cement and concrete industry [58]. Application of microwave heating in the chemical industry is relatively a new field, with only a limited number of review articles being available. These review articles either deal with specific areas of chemical engineering, such as catalytic reactions and chemical separation [59] or provide a broad overview of applications of microwave heating in chemical engineering processes [47]. A comprehensive analysis of the recent literature on microwave-heated multiphase reactors, such as fixed beds, structured beds, and slurries, is missing. This review article fills this critical gap by focusing on both experimental and modeling studies of microwave

multiphase reactors in a holistic manner. We also discuss the major trends and future directions for microwave-assisted process intensification.

The remainder of the paper is organized into four sections. Section 2 provides a brief background on microwave heating mechanisms and temperature measurements to help the reader understand the later sections. Experimental investigations are reviewed in Section 3, while Section 4 deals with the modeling and simulation of microwave multiphase reactors. Recent simulation studies are summarized, and the need for multiscale modeling to deal with the complexity and computational cost of simulations is discussed. Finally, Section 5 concludes the paper with major trends and future directions.

2. Fundamentals of microwave heating

For a detailed background of the fundamentals of microwave heating, we refer the readers to the textbook by Pozar [60] and previous review papers [47, 50, 61]. Here, we provide a brief background on microwave heating, relevant for the following sections. Microwave radiation is a part of the electromagnetic spectrum in the 300 MHz - 300 GHz frequency range. The Federal Communication Commission (FCC) has allotted specific frequencies for Industrial, Scientific, Medical and Instrumentation (ISMI) applications to avoid the potential interference between the communication and heating applications. The most utilized frequencies for microwave heating are 2.45 GHz and 915 MHz. Kitchen and lab-scale microwave ovens generally operate at a frequency of 2.45 GHz corresponding to a wavelength of 12.2 cm in air, whereas 915 MHz is more common in industrial microwave heating applications with a wavelength of 32.7 cm

in air. The conversion efficiency of electricity into microwaves is also higher for 915 MHz (approximately 85%) compared to 2.45 GHz (approximately 50%) [62, 63].

Microwaves generate heat in materials through various mechanisms leading to selective heating in multiphase systems consisting of different materials. Most of the unique features observed in microwave heated multiphase reactors can be related to this selective heating. Since many of the reactions, having high activation energy, are strong functions of temperature, accurate temperature measurement is essential. However, the interaction of microwaves with thermocouples makes temperature measurement a challenge. The next two subsections summarize important heating mechanisms of microwaves and temperature measurement techniques and challenges during microwave heating.

2.1 Microwave heating mechanisms

Microwave heating results from the direct interaction of microwaves with a material. Based on the interaction of the electric and magnetic fields with materials, different heating mechanisms occur. The electric field is mainly responsible for the dielectric heating through dipolar polarization, ionic conduction, and Maxwell-Wagner polarization [64]. In dipolar polarization, microwaves cause a rotational motion of the permanent or induced dipoles. Upon microwave irradiation, dipoles try to align in the oscillating electric field direction and experience resistance due to inter-particle and inter-molecular interactions generating random motion of the molecules, resulting in volumetric heating of the material [65]. Polar liquids, such as water, are heated through dipolar polarization. In the ionic conduction mechanism, the microwave irradiation creates an oscillating electric current in a material via the translational motion of

mobile charge carriers, such as ions and electrons. Here, heat generation depends on the material resistivity as in the case of Joule heating. Ionic liquids are heated through this mechanism. In certain dielectric solid materials, charged particles, such as $\pi-$ electrons, move with the oscillating electric field in a delimited region. Energy is dissipated in the form of heat as the electrons fail to couple with the rapidly changing phase of the electric field. This effect known as the Maxwell-Wagner polarization can be observed in microwave heating of carbon materials.

Heating due to the magnetic field of magnetic materials is less common in chemical engineering applications. Three primary mechanisms are eddy current losses, hysteresis losses, and magnetic resonance losses or residual losses. Eddy current loss is essentially Joule heating caused by the magnetic field induced eddy current. The hysteresis losses originate from the rapid flipping of the magnetic domains and its resultant friction. The magnetic resonance losses/residual losses are induced by domain wall resonance and electron spin resonance. Refs. [64, 66] review various microwave heating mechanisms in detail.

The permittivity ε and permeability μ, which are complex numbers, quantify a material's ability to store and dissipate the energy of the electric and magnetic fields, respectively. In practice, the relative permittivity, $\varepsilon_r = \varepsilon/\varepsilon_0 = \varepsilon' - j\,\varepsilon''$, and the relative permeability, $\mu_r = \mu/\mu_0 = \mu' - j\mu''$, are reported instead of ε and μ. Here $\varepsilon_0 = 8.854 \times 10^{-12}$ F/m and $\mu_0 = 4\pi \times 10^{-7}$ H/m are the permittivity and permeability of the free space, respectively. ε', the real part of ε_r, is commonly known as the dielectric constant and quantifies the ability of the material to store the electrical energy, whereas ε'', the imaginary part of ε_r, is commonly known as the dielectric loss factor and describes the material's ability to dissipate the stored electric energy into heat. Physically ε' is related to the material's ability to create dipoles, ions, and free

electrons, whereas ε'' is related to the resistance experienced during the motion of the charged entities by the oscillating microwaves. μ' and μ'' are analogous to ε' and ε'' for a magnetic field. The ability of a material to be heated under microwave irradiation is quantified by the electric loss tangent $\tan\delta_e = \varepsilon''/\varepsilon'$ and the magnetic loss tangent $\tan\delta_m = \mu''/\mu'$. Higher values of $\tan\delta_e$ and $\tan\delta_m$ are associated with a higher propensity toward microwave heating.

The permittivity and permeability affect the distribution of the electromagnetic field in a cavity and can vary significantly with temperature. For example, the loss factor of silicon carbide increases from 1.71 to 27.99 from room temperature to 695 ℃ at the microwave frequency of 2.45 GHz [66]. Since most of the materials used in chemical engineering applications are non-magnetic, the knowledge of permittivity as a function of temperature is sufficient. One interesting application not fully exploited is the use of magnetic field for ferromagnetic catalyst nanoparticles. Permittivity also affects the microwaves' ability for volumetric heating, which can be quantified using penetration depth, defined as the distance at which the electromagnetic field's power decreases to 1/e (~37%) of its incident value. Table 1 provides the permittivity and penetration depth of commonly used liquids and solids at room temperature at a microwave frequency of 2.45 GHz.

In a multiphase system where one phase is a strong microwave absorber, such as activated carbon, silicon carbide or water, and the other phase is not, such as gas or liquid toluene, selective heating occurs. This selective heating is a key principle for process intensification of microwave multiphase reactors. Recently, a few experimental and simulation studies have investigated this mechanism quantitatively [43, 67, 68]. For example, Goyal et al. [67] showed that the microwave heating rate of slurries can be tuned by selecting solids with

different permittivity. Malhotra et al. [43] quantified the conditions required to maintain a temperature difference between the gas and solid phases of a monolith. More fundamental studies are needed to build design principles to estimate the temperature difference between the phases of a multiphase microwave reactor. A detailed description of microwave heating mechanisms can be found in Ref. [64, 66].

Table 1: The relative permittivity and penetration depth of common materials utilized in chemical engineering applications at room temperature and 2.45 GHz frequency.

Material	Relative permittivity [-]	Penetration depth [m]
Solids [20, 66, 69, 70]		
Alumina	9-0.0063j	9.28
Carbon nanotube	18-30j	0.0027
Cordierite	1.5-0.007j	3.41
Co/SiO_2	9.87-2.09j	0.029
Ga/Al_2O_3	9.17-0.48j	0.12
Glass	4.82-0.026j	1.65
MgO	9-0.0045j	12.99
Natural Rubber	2.2-0.01j	2.89
Polystyrene	2.55-0.0008j	38.90
PTFE	2.08-0.0008j	35.13
PVC	2.85-0.016j	2.06

Quartz	4-0.001j	39.98
Silicon carbide	9.72-2.01j	0.03
Soda lime glass	6-1.2j	0.039
Styrofoam	1.03-0.0001j	197.78
Teflon	2.1-0.001j	28.24
TiO_2	50-0.25j	0.55
ZrO_2	20-2j	0.044
Liquids [41, 44, 69, 71-74]		
Water	78.0-10.5j	0.016
Acetone	18.11-9.02j	0.0092
Acetonitrile	36.69-1.52j	0.078
Ethanol	6.6-6.30j	0.0079
Hexane	1.9-0.03j	0.89
Methanol	32.6-21.48j	0.0052
Methyl isobutyl ketone	13.41-2.08j	0.034
Propylene Carbonate	60.12-19.91j	0.0076
Tetrahydrofuran	8.25-0.55j	0.10
Toluene	2.4-0.096j	0.31
2-Methyltetrahydrofuran	8.67-1.40j	0.04
γ-valerolactone	33.15-11.20j	0.01

2.2 Temperature measurement during microwave heating

Accurate measurement of the temperature field within a microwave reactor is a complex and challenging task. Thermocouples, widely used for temperature measurements in conventional heating, cannot easily be used. The interaction between microwaves and metallic thermocouples enhances the electromagnetic field strength locally around the thermocouple, sometimes dramatically enough to induce dielectric breakdown and the ensuing safety hazards. The locally-intensified electromagnetic field creates temperature gradients large enough to render the local temperature measurement wholly inadequate [75, 76]. Thermocouples with insulation have been used during microwave heating [31, 77-79]. However, the accuracy of those measurements is not verified.

Optical fiber, pyrometer, and infrared (IR) thermal camera are the most common temperature measurement instruments for microwave heating. Most optical fiber-based temperature measurements exploit the temperature dependence of the bandgap of semiconductor crystals, such as gallium arsenide (GaAs). All the optical fiber components are non-metallic and do not interfere with microwaves; therefore, optical fibers can measure the temperature inside a microwave reactor at a local point. In contrast, pyrometer and thermal camera measure surface temperatures over a fixed area, yielding a spot measurement or a surface mapping of temperature, respectively. While optical fibers are generally limited to temperatures below 300 ℃, pyrometers and thermal cameras are often used to measure temperatures over 1000 ℃ [80]. Pyrometer and thermal camera indirectly measure the temperature field based on the Stefan-Boltzmann law and requires knowledge of the emissivity of the reactor surface and other media between the thermal camera and the reactor surface, such as a glass window. Magnetic Resonance Imaging (MRI) has also been used to measure the

three-dimensional temperature field during microwave heating, especially in food applications. Using MRI, good spatial resolution (~mm) is attained for the surface temperature and the temperature within the material. However, the exorbitant cost of MRI tomographs and the requirement of unbounded water in the material have limited its widespread usage [81].

As optical fibers, pyrometers, and thermal cameras provide the local and surface temperature, accurate temperature field within the microwave reactor cannot be obtained. This is a major shortcoming of the microwave heating experiments and has hindered a comprehensive understanding of the impact of microwaves on chemical transformations.

3. Process intensification in microwave multiphase systems

Multiphase reactors can be divided into two major classes based on the phases (fluid or solid) involved: fluid-fluid (dispersed and biphasic) and fluid-solid (slurry, fixed bed, and structured bed) systems. The next two subsections review the recent experimental work on microwave heated multiphase reactors with a focus on challenges and opportunities in achieving process intensification using microwaves.

3.1 *Fluid-fluid systems*

Fluid-fluid systems typically entail two immiscible fluids in contact with each other, where the difference in the dielectric properties of the two phases results in selective microwave heating. Here one phase can be dispersed in the other or two bulk phases with a single interface can form as shown in Figure 1. The former is widely used in emulsion polymerization of various monomers [82-84] and the latter for reactive extraction applications [85-87], such as in biomass

conversion. Several examples are listed in Table 2. Both systems are described in the next two subsections.

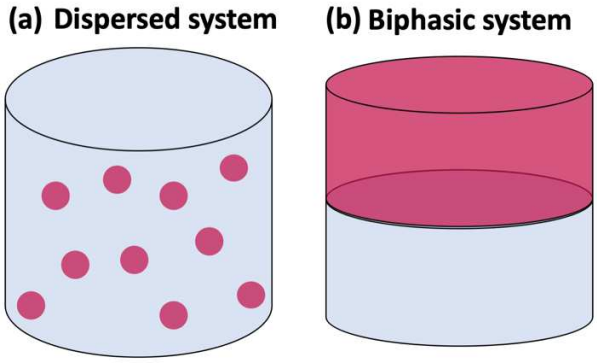

Figure 1. Schematic of the two extreme mixing cases of fluid-fluid systems.

3.1.1 Dispersed systems

The most common application of microwave heating of liquid-liquid dispersed systems is emulsion polymerization; several reviews on this topic exist [82-84]. Since microwave heating depends on the dielectric properties of a material, the rate and product distribution of emulsion polymerization is sensitive to the dielectric properties of monomers and solvents [88]. For example, in [89] the emulsion copolymerization of butyl acrylate (higher dipole moment) and styrene (lower dipole moment), heating of the monomer droplets leads to a sharp increase in the reactivity of butyl acrylate and a more uniform particle size. This result can be partly attributed to particle fragmentation due to a hotter region at the particle surface leading to further reduction of the interfacial tension [90], and partly to shorter time to coagulate owing to the faster reaction kinetics [91]. Also, a higher processing rate can be achieved under rapid

microwave heating. For example, in emulsion polymerization of styrene, microwave heating required less than half the time of conventional heating to reach 95% yield of polystyrene [26].

Apart from dispersed liquid phases, limited amount of work has also been applied to gas bubbles dispersed in a liquid [6]. Bruyn et al. [6] investigated the impact of microwave heating on (3-methoxyphenyl) methylammonium bromide into (3-hydroxyphenyl) methylammonium bromide, a demethylation reaction relevant to the pharmaceutical industry. COMSOL simulations revealed that a sharp variation in the dielectric properties across the interface concentrates the electric field there, resulting in much higher electromagnetic energy dissipation near the gas-liquid interface (see Figure 2). This unique heating of liquid near bubbles resulted in a large number of bubbles leading to rapid elimination of gaseous byproducts, thereby changing the observed reaction order of the demethylation reaction from two to zero.

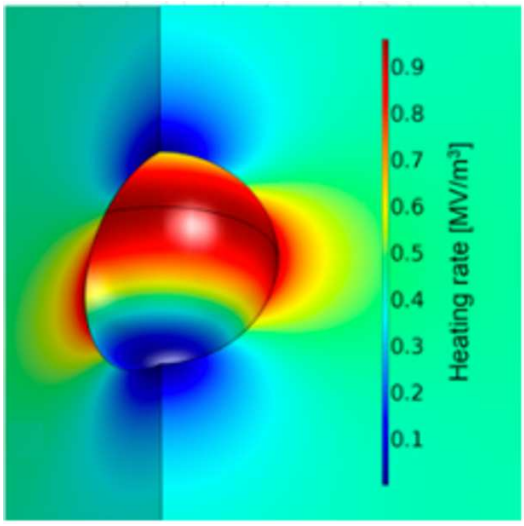

Figure 2. Simulated heating rate around a bubble. Regions of high heating rate occur in the vicinity of the bubble. (Reprinted with permission from the publisher; Bruyn et al. [6]).

3.1.2 *Biphasic systems*

Microwave heating has also been applied to biphasic systems (Figure 1 b). Here two bulk immiscible liquids of different dielectric properties result in a temperature gradient between them under microwave irradiation. Figure 3 shows the predicted temperature field obtained from COMSOL simulations conducted here of a water-MIBK biphasic system. Water being a better microwave susceptor undergoes faster microwave heating than MIBK, resulting in a temperature gradient between the two liquids. Selective microwave heating of one phase in conjunction with the temperature dependent solute solubility can play a crucial role in reactive extraction. These characteristics have been exploited in biphasic immiscible organic and aqueous systems for the conversion of biomass-derived cellulose and sugars, such as glucose and xylose, into platform chemicals, such as hydroxymethyl furfural (HMF) [85-87].

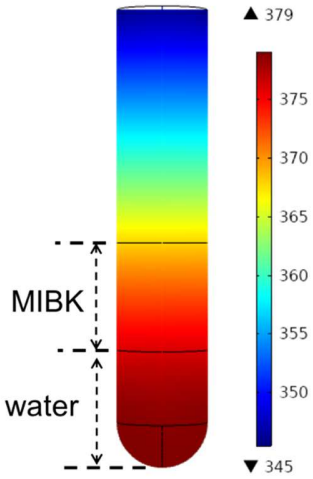

Figure 3. Simulated temperature field in microwave heating of 1.5 mL water (bottom liquid) and 1.5 mL MIBK (top liquid) in a 10 mL Pyrex vial in the CEM Discover reactor. Sharp temperature difference is observed. Color bar represents the temperature scale in Kelvin.

In situ extraction of the product from the aqueous to the organic phase reduces the byproduct formation and thus improves the selectivity [92]. For example, the yield and selectivity

of 5-chloromethylfurfural (CMF) increased from 75% to 85% and 96% to 98%, respectively, by reducing undesirable humins from glucose, fructose, and cellulose using a water/ethylene dichloride biphasic system under microwave irradiation [92]. The lower polarity of ethylene dichloride (ε_r=10.36-1.11j) leads to the selective microwave heating of the aqueous phase (ε_r=78.0-10.5j). The higher temperature of the aqueous phase favors CMF formation, while the lower temperature of ethylene dichloride favors the extraction of CMF, thereby reducing the conversion of CMF into humins. By tuning the ratio of the dieletctric constants of aqueous and organic phases, the temperature gradient can be optimized to maximize the product yield [27].

Though the improvement in reaction time, yield, and selectivity has been widely reported and attributed to the difference of dielectric properties, a quantitative analysis is still missing. The performance of the reactive extraction is sensitive to the temperature difference between the two phases as material properties and process parameters, such as miscibility, partition coefficient, permittivity, diffusivities, and viscosities, depend on temperature. However, none of the works has directly measured the temperature of both phases to rationalize the advantage of selective heating. Further investigations on how the temperature difference correlates to material properties are needed. Further, we hypothesize that the temperature difference depends on the geometric factors, such as volumes of phases that controls conductive heat transfer. Beyond fundamental understanding of the system, optimal selection of organic solvents becomes a daunting task and requires high throughput computational design tools. Such tools are not available at present and require further methodological work. We purpose that multiscale modeling and data science tools can open up new venues of research. It is also unclear

how much the performance can be improved by solvent and process condition optimization. Setting up ideal performance targets is thus an important task for future work.

Application of microwave heating to fluid-fluid systems has been limited. The intensification observed in emulsion polymerization and reactive extraction could be replicated in other areas where the conversion process is sensitive to selective or rapid heating. Moreover, most of the fluid-fluid reactor studies have been conducted in batch; exploiting microwave-assisted continuous-flow reactors can lead to further process intensification.

3.2 *Fluid-solid systems*

Majority of the applications of microwave heating in multiphase systems target fluid-solid systems with a focus on heterogeneous catalytic reactors. Heterogeneous catalysis plays an essential role across the chemical industry. Increased reactant conversion with reduced reaction time can be achieved thanks to the rapid and selective microwave heating. Selective microwave heating can create a temperature gradient with a “hot” solid catalyst and a “cold” fluid, suppressing the homogeneous gas phase reactions while maintaining high catalyst activity. As a result, higher selectivity to the desired products can be achieved compared to conventional heating. Several examples are listed in Table 2. In the following subsections, we review the application of microwave heating to fluid-solid multiphase reactor configurations, namely slurry, fixed bed, and structured bed reactors. A schematic of these configurations is shown in Figure 4.

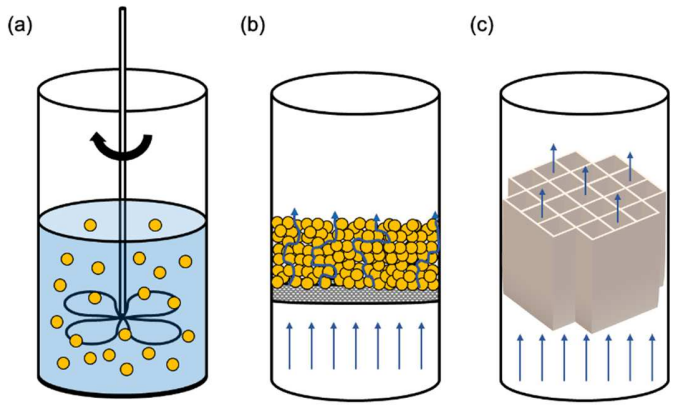

Figure 4. Three major categories of solid-fluid reactors utilized in microwave heating: (a) Slurry reactor; (b) Fixed bed reactor; (c) Structured bed reactor.

3.2.1 *Slurry reactors*

A common slurry reactor consists of solid particles dispersed in a liquid (continuum phase). In microwave heated slurries, a microwave transparent liquid, such as toluene ($\varepsilon_r = 2.4 - 0.096j$), and a strongly microwave absorbing dispersed phase, such as activated carbon ($\varepsilon_r = 35 - 1.1j$), are employed. Dissipation of microwave energy occurs in the dispersed phase and depending on the slurry hydrodynamics, a temperature gradient can exist between the dispersed and continuum phases [67]. Only a few investigations of microwave heated slurries have been carried out; most of them are conducted by Horikoshi and co-workers targeting the Suzuki–Miyaura cross-coupling reaction [7, 10-12, 14] and tetralin dehydrogenation [11, 15, 16]. For both the reactions, a slurry of activated carbon (AC) granules dispersed in toluene was used. AC is used as a catalyst support with platinum (Pt) and palladium (Pd) as the active metal for Suzuki–Miyaura cross-coupling reaction and tetralin dehydrogenation, respectively.

These studies elucidated the impact of the electric and magnetic field on selective heating, generation of hot spots and arcing, and the reaction performance. For this purpose, the reaction vial was kept at the locations of the maximum electric and magnetic fields. Both the electric and magnetic fields selectively heat the activated carbon. However, hot spots were observed at lower microwave power (< 200 W) in the electric field compared to the magnetic field (>200 W) due to the different heating mechanisms of the electric and magnetic fields. The electric field heats the activated carbon through Joule heating, whereas the magnetic field creates eddy current and causes induction heating. The need of higher power to create hot spots under the magnetic field points to the lower tendency of the magnetic field to accumulate the π −electrons near the sharp edges of the activated carbon particles. This accumulation of the π −electrons may cause highly concentrated electric filed, which can become higher than the dielectric strength (∼3 KV/mm for air) leading to electric sparks or arcing. Arcing and hot spots can cause the high temperature and sintering (∼10 nm to ∼100 nm), reducing the catalytic activity.

Heating in the magnetic field provided higher product yield than in an electric field or oil-bath [7, 10]. We hypothesize that the circular eddy currents generated by the magnetic field lead to a more uniform distribution of π − electrons on the activated carbon than the electric field. However, even with the same microwave cavity and reaction vial, the electric field provided a higher product yield than the oil-bath in some studies [10, 11] and lower in others [7, 12, 14]. These contradictory findings show that the performance of microwave heating is sensitive to small experimental differences. In contrast, tetralin conversion was significantly higher under microwave heating even with hot spots than in a conventionally heated reactor [11]. This observation could be related to the difference between the melting points of platinum (1768 ℃)

and palladium (1555 ℃). The higher melting point of platinum, used in tetralin dehydrogenation, lowers the potential of forming metal aggregates due to hot spot formation and maintains the catalyst activity. More work is required to quantify these effects and exploit them for engineering applications.

A few strategies have been suggested to reduce hot spot formation in slurries including the use of a magnetic field, carbon microcoils as a catalyst support, or polar solvent, and variation in the size of the reaction vessel and stirring rate. For the Suzuki-Miyaura reaction, carbon microcoils formed no hot spots and provided 70% higher yield of the product (4-methylbiphenyl) compared to the activated carbon, despite their lower specific surface area [11]. The large size and smoother surface of the microcoils provided a more uniform heating compared to the activated carbon granules and suppressed hot spot formation leading to better reaction performance. Figure 5 shows that high stirring rate, e.g., 1500 rpm, substantially suppresses hot spot formation [93]. At high stirring rates, heat transfer from the particles to the liquid increases as well as the distribution of the particles become more [67]. Moreover, indirect heating of particles reduces hot spot formation. For example, using a Dewar-like reactor filled with an organic solvent and a microwave absorbing material reduces the direct heating of activated carbon and thus the hot spot formation [12].

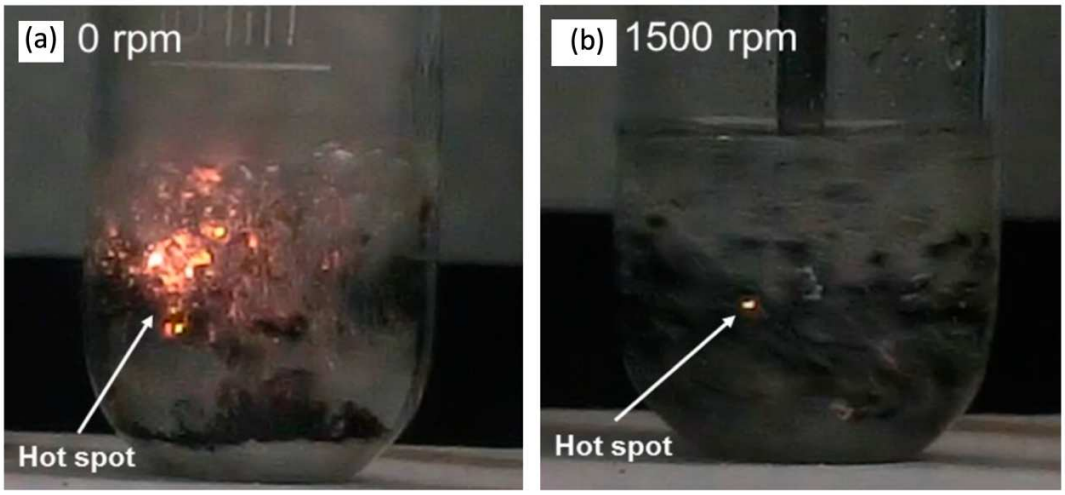

Figure 5: High-speed camera images of hot spots generated in a slurry undergoing microwave heating. (a) No stirring; (b) Stirring at 1500 rpm (Reprinted with permission from the publisher; Horikoshi et al. [93]*).*

The sensitivity of the slurry reactor performance in microwave heating makes it challenging to quantify the microwave process-intensification potential. For example, as the catalyst loading increase, so does the potential for arcing. Moreover, magnetrons or semiconductor generators can result in dissimilar heating patterns leading to different reaction performance [10]. Semiconductor generators provide a narrower range of microwave frequencies compared to a magnetron. Investigations with controlled experimental and computational parameters are essential in quantifying the potential of microwave heating in slurry reactors. There is a clear need for techniques and methods to simultaneously provide the temperature of the particles and of the liquid during microwave heating and for criteria to suppress arcing. In a recent contribution [67], we proposed engineering criteria to do so.

3.2.2 *Fixed bed reactors*

Most microwave multiphase reactors focus on catalytic fixed bed reactors, a classic configuration used for over a century in the chemical industry. Apart from catalytic reactions, microwave heated fixed beds have also found applications in the pyrolysis of biomass, coal, and shale [94]. Many of these materials are poor in dissipating microwave energy; therefore, metal oxides and carbon materials are used as susceptors. Like slurries, fixed beds undergo selective heating and hot spot formation. The higher temperature of the solid favors catalytic reactions over the gas-phase reactions.

Higher yield and selectivity have been observed for ethane dehydroaromatization [32], conversion of ethane to ethylene [95], and dehydrogenation of tetralin [23], 2-propanol [24], and ethylbenzene [96]. However, extending the superior performance to other chemistries has been elusive. For instance, microwave-heated tetralin dehydrogenation achieved 20% higher conversion and lower coke compared to conventional heating [23]. However, with the same reactor setup, such an enhancement was not observed for decalin dehydrogenation. In these experiments, a fixed bed reactor of activated carbon granules of size 0.71-1.4 mm was used with Pt for tetralin dehydrogenation and Pt-Sn for decalin dehydrogenation. The authors proposed that the temperature gradient between the catalyst particles and the surrounding liquid leads to an enhanced desorption of the naphthalene, which is a precursor to coke formation. Tetralin dehydrogenation is controlled by desorption and decalin dehydrogenation is not. Thus, enhancement in the mass transfer rate favors tetralin dehydrogenation. In these studies, the catalyst and liquid temperatures and the mass transfer rate are not measured, so direct evidence

is lacking. These results indicate that the reaction performance depends on the microwave-induced thermal-gradient and desorption.

Figure 6 shows hot spot formation during microwave heating of silicon carbide spheres (with diameters of 2.38, 3.18, and 3.97 mm) in contact with each other [24]. Temperature higher than the bulk sphere temperature confined to a small region (~0.5 mm) around the contact point is observed. The temperature difference increased from 150 ℃ to 240 ℃ as the sphere diameter increased from 2.38 mm to 3.97 mm, implying the competition between conduction and heat generation. Both experiments and computations [7] have shown that electric field gets concentrated in a narrow region between two strong microwave absorbers, such as silicon carbide and activated carbon. In fixed beds, the contact points between particles or pellets provide ideal conditions for hot spots. Effective strategies are needed to control hot spot formation before the lab-scale success can be implemented at large scales. We discuss such a possibility below.

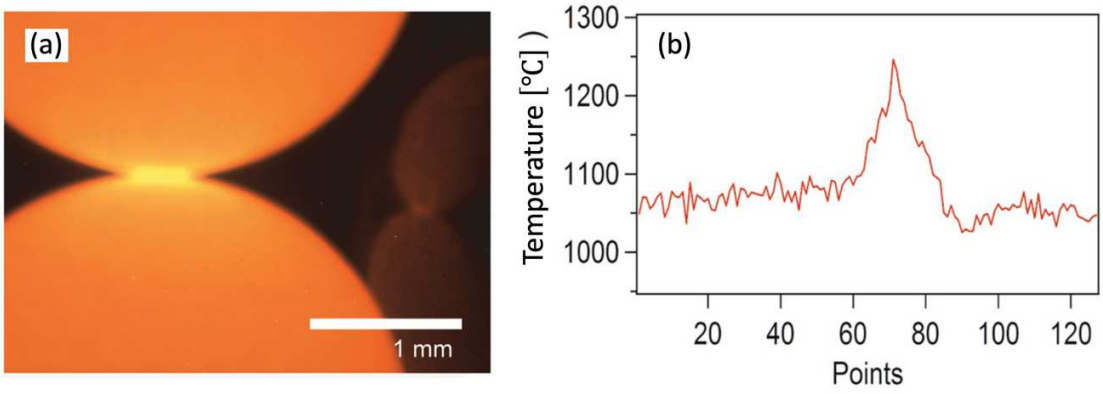

Figure 6: (a) Image of a hot spot at the contact point between two silicon carbide particles of diameter 2.38 mm captured using in-situ spectroscopy. (b) Temperature distribution corresponding to the image in (a). (Reprinted with permission from the publisher; Haneishi et al. [24]).

Most of the recent studies attribute the observed differences between the microwave and conventional heating in fixed beds to the non-uniform temperature distribution and hot spot formation. A 2009 review article [97] reported that the number of publications reporting microwave-specific (non-thermal) effect has significantly reduced. However, even today, some studies suggest a reduction in the activation energy for the enhancement of reaction performance under microwave irradiation. For instance, Xu et al. [31] challenged the prevalent hypothesis of selective heating and hot spot formation and postulated a decrease in the apparent activation energy for the catalytic decomposition of NO. The authors assumed that the maximum temperature of the catalyst bed can be 200 ℃ higher than the experimentally measured value. The yield calculated at this higher temperature is still lower than the experimentally obtained yield. Large temperature variations can exist in both the horizontal (～140 ℃) and vertical directions (～250 ℃) with the core temperature of 600 ℃ in a fixed bed [96]. However, in the experiments of Xu et al. [31], the temperature was measured only at a single location using a thermocouple. Accurate measurements of the temperature profile inside a fixed bed during microwave heating is imperative for a clear understanding of the underlying processes.

In summary, even though laboratory and industrial fixed beds are commonplace, hot spots severely limit their application. We postulate that the temperature difference between the solid and the fluid is small due to the small gap between the particles and spatially varying due to random packing. Experimental and simulation studies of the temperature field are challenging.

3.2.3 Structured Reactors

For a comprehensive review of the older literature on microwave heating of heterogeneous catalytic reactions in fixed beds, we refer to the papers by Stankiewicz and co-workers [97] and Horikoshi and co-workers [50]. The non-uniform temperature distribution and hot spot formation in fixed beds can be alleviated using structured reactors (Figure 4c), which also offer smaller pressure drop and enhanced heat and mass transfer rates [98]. For the same material, structured reactors offer excellent heat conduction properties compared to fixed beds [99]. This enhanced heat transfer and their monolithic nature help in suppressing hot spots and achieving a more uniform temperature. Catalyst coated monoliths and open-cell foams made of silicon carbide or cordierite are the most common in microwave heating. Silicon carbide is a strong heat conductor (up to 400 W/m.K) and microwave susceptor ($\varepsilon_r = 9.72\text{-}2.01j$), whereas cordierite offers low thermal conductivity (up to 3 W/m·K) and is a poor microwave susceptor ($\varepsilon_r = 1.5\text{-}0.007j$). Therefore, microwave heating of a cordierite-based reactor relies on the dielectric properties of the catalyst coating. For example, the loss tangent of a cordierite monolith increases from 0.004 to 0.020 after coating it with silver-copper oxide ($\tan\delta_e = 1.029$) catalyst [20].

In recent years, several studies have demonstrated the process intensification potential of microwave heated structured reactors for enhanced product selectivity and production rate. Examples include valorization of low molecular weight alkanes [5, 19, 22, 100, 101] and ethylene epoxidation [20, 21]. Like other fluid-solid reactors, this enhanced performance can be explained by the temperature gradient between the solid and fluid phases. Santamaria and co-workers [5, 19-21] measured the temperature of each phase separately and confirmed that indeed the solid is hotter than the gas using a calibrated IR pyrometer and thermocouples simultaneously. For

example, in ethylene epoxidation over cordierite monoliths coated with a silver-copper oxide catalyst, a temperature difference of 50 ℃ was observed with the solid at 200 ℃ [21].

The performance of a structured reactor is sensitive to the uniformity of the catalyst coating, especially in the case of cordierite, which is a poor microwave susceptor and microwave heating occurs due to catalyst coating. For instance, the inhomogeneity of catalyst coating on a cordierite monolith led to formation of hot spots decreasing the selectivity in ethylene epoxidation [20] and non-oxidative methane coupling [100]. A thicker catalyst coating heats preferentially leading to hot spot formation and a boost of reactivity, resulting in inhomogeneous accumulation of side products, such as coke. Coke disturbs the microwave field leading to microwave decoupling. Over a silicon carbide monolith, a more uniform temperature profile can be obtained even with an irregular catalyst coating [70].

In the above mentioned studies, a substantial temperature difference is observed between the solid and gas phases due to the selective microwave heating of the solid. The higher temperature of the solid catalyst compared to the gas-phase enhances the rate of catalytic reaction and suppresses the gas-phase side reactions resulting in a significant intensification of yield and selectivity. Besides, enhanced heat transfer due to the geometry of the structured reactors as well as the absence of contact points eliminate hot spots. Thus, microwave heated structured reactors are superior to fixed beds. At present, silicon carbide-based monoliths are an ideal structured reactor. However, exploration of novel materials as well as geometries could diversify the portfolio of structured reactors. Besides the application in chemical transformations, structured reactors have also been utilized in hydrogen release from metal hydrides [102]. Such investigations are few. All the studies here involve solids and gases. It is worth exploring reactions

of liquid feeds in structured reactors. One of the successful examples is the use of $CoFe_2O_4$/SiC foam under microwave radiation for the rapid degradation of malachite green, an organic pollutant [103]. Clearly, understanding how to tune the solid-fluid temperature difference as a function of operating conditions and materials is an important future direction. The recent introduction of fixed bed micro monoliths improves catalyst loading, allows flexibility in material selection, and eliminates hot spots [68]. Additive manufacturing enables production of complex structures that can be leveraged for microwave heated reactors.

Table 2: Summary of reactions studied and major observations for various multiphase reactors heated conventionally and via microwaves. CH and MWH refer to conventional and microwave heating, respectively. X_i, Y_i, and S_i refer to conversion, yield, and selectivity of species i, respectively. Note that the temperature values correspond to the local temperature measured with an optical fiber or pyrometer or the average of thermal camera measurements. These temperature values are maintained by controlling the microwave power output using a control unit.

Reaction	**Catalyst and reaction temperature**	**Conversion/selectivity/yield**		**Other differences**	**Explanation for observations during MWH**
		Conventional	**Microwave**		
Biphasic systems					
Fructose conversion to 5-	HCl; 80 ℃	Y: 75%; S: 96%	Y: 85%; S: 98%	-	Selective heating of the acidic aqueous layer

chloromethyl furfural [92]					
Xylan conversion to furfural [72]	$Al_2(SO_4)_3$; 130 ℃	Y: 70%	Y: 87.8%	Reaction time of 5 h and 30 min for CH and MHW, respectively	Faster reaction kinetics at high reaction temperature resulting from rapid heating
Xylose conversion to furfural [27]	H_2SO_4; 200 ℃	Y: 65%	Y: 80%	50% reduction in byproducts under MWH	Selective heating of reactive aqueous phase
Fructose dehydration to hydroxymethylfurfural [104]	HCl; 160 ℃	X: 94%; Y: 79%; S: 85%	X: 99%; Y: 91%; S: 92%	Reaction time of 40 and 1 min for CH and MWH, respectively	Rapid heating leading to faster kinetics and reducing product decomposition time
Dispersed systems					

Dispersion copolymerization of 2-ethylhexyl methacrylate and vinylbenzyl chloride [91]	- 50 - 70 ℃	-	-	Particles did not coagulate under MWH; Reaction time was 24 h and 5 h for CH and MWH, respectively	Faster reaction kinetics and possibly more uniform and fast heating of the internal volumes of the particles to prevent coagulation
Emulsion polymerization of styrene [26]	- 65 - 85 ℃	Y: 95%	Y: 95%	Reaction time was 90 min and 40 min for CH and MWH, respectively	Faster reaction kinetics resulting from rapid heating
Structured reactors					
Methane non-oxidative coupling [5]	Mo/ZSM5; 700 ℃	X_{CH4}: 10.1%; Y_{coke}: 5.49 wt%	X_{CH4}: 11.0%; Y_{coke}: 2.2 wt%	Higher selectivity and less coke during MWH	Altered formation of the active catalytic species of Mo_2C; Gas-solid

					temperature gradient prevents formation of coke from PAHs in the gas phase
Oxidative dehydrogenation of isobutane with CO_2 [19]	V/Al_2O_3; 575-675 ℃	$Y_{isobutylene}$: 25.3%; $S_{isobutylene}$: 45.8%	$Y_{isobutylene}$: 28.7%; $S_{isobutylene}$: 76.5%	-	Selective heating leads to temperature difference between gas and solid reducing the homogeneous gas-phase reaction
Ethylene epoxidation [20]	Epoxidation catalyst; 125-225 ℃	$X_{ethylene}$: 10% and $S_{ethylene-oxide}$:65% for both homogeneous and inhomogeneo	$X_{ethylene}$: 10% and $S_{ethylene-oxide}$:65% for homogeneo us coating of catalyst;	For equal ethylene conversion, MWH provides lower gas phase temperature	Selective heating leads to temperature difference between gas and solid; Formation of hot spots due to

		us coating of catalyst	$X_{ethylene}$: 20% and $S_{ethylene-oxide}$:35% for inhomogeneous coating of catalyst	compared to CH	inhomogeneous coating of catalyst
Hydrogen release from hydrides [102]	- Up to 120 ℃	N/A	N/A	High energy efficiency (90%) under MWH, 3.3 times higher than by CH	Inverse temperature profile is obtained during MWH leading to lower heat losses compared to CH where the reactor surface temperature is higher

Propane dehydrogenation [22]	VMgO; 525-600 ℃	$X_{propane}$: 38%; $S_{proplyene}$: 53%	$X_{propane}$: 21%; $S_{proplyene}$: 70%	-	Selective heating leads to temperature difference between gas and solid reducing the homogeneous gas-phase reaction
Slurry					
Suzuki–Miyaura cross-coupling [10]	Pd/AC; 110 ℃	$Y_{methylbiphenyl}$: 2.8%	$Y_{methylbiphenyl}$: 11.8% under electric field conditions; $Y_{methylbiphenyl}$: 22.1% under magnetic field conditions	Hot spots are observed during MWH under maximal electric field condition	Hot spots form under the maximal electric field conditions but not with the magnetic field; Deactivation of the Pd catalyst due to hot spots; Higher catalyst temperature

					compared to the solvent
Suzuki–Miyaura cross-coupling [11]	Pd/AC and Pd/carbon microcoils; 70 - 110 ℃	$Y_{methylbiphenyl}$: 14% using Pd/ carbon microcoils; $Y_{methylbiphenyl}$: 17% using Pd/AC	$Y_{methylbiphenyl}$: 38% using Pd/ carbon microcoils; $Y_{methylbiphenyl}$: 23% using Pd/AC	Hot spots are observed during MWH of AC	Faster heating with carbon microcoils compared to AC; No hot spot formation with carbon microcoils due to their helical structure and lower electrical conductivity compared to AC
Suzuki–Miyaura	Pd/AC; 50 - 113 ℃	$Y_{methylbiphenyl}$: 18.7%	$Y_{methylbiphenyl}$: 34.2% utilizing	Hot spots at 70 W and 200 W with	Hot spots formation under direct MWH;

cross-coupling [12]			microwave-absorber heating stick at 70 W; $Y_{methylbiphenyl}$: 10.2% at 200 W	and without utilizing microwave-absorber heating sticks, respectively	Pd catalyst deactivation due to hot spots; Lower heat losses and suppression of hot spots while utilizing microwave-absorber heating sticks
Suzuki–Miyaura cross-coupling [7]	Pd/AC; < 400 °C	$Y_{methylbiphenyl}$: 21.3%	$Y_{methylbiphenyl}$: 5.7% under electric field; $Y_{methylbiphenyl}$: 34% under magnetic field	Hot spots are observed during MWH under maximal electric field condition	Hot spots under the maximal electric field conditions but not with the magnetic field; Pd catalyst deactivation due to hot spots; Higher catalyst temperature

					compared to the solvent
Suzuki–Miyaura cross-coupling reaction [14]	Pd/AC; 120 ℃	$Y_{methylbiphenyl}$: 43%	$Y_{methylbiphenyl}$: 40% with 1000 W; $Y_{methylbiphenyl}$: 35% with 500 W	Hot spots during MWH	Inactivation of the Pd catalyst due to hot spots formation under MWH
Tetralin dehydrogenation [15]	Pt/AC; 207 ℃	$X_{tetralin}$: 31.6% at 207 °C	$X_{tetralin}$: 50.1%	Lower retardation constant	Selective heating of catalyst during MWH facilitates the desorption of naphthalene
Tetralin dehydrogenation [16]	Pt/AC; 220 ℃	N/A	$X_{tetralin}$: 56% in Dewar-like insulation reactor (DIR)	Higher conversion of tetralin in DIR compared to CNR	Lower heat loss in DIR compared to CNR
			$X_{tetralin}$: 31% in		

			Conventional non-insulated reactor (CNR)		
Fixed bed					
Direct ethane dehydroaromatization [32]	Mo-M/ZSM5; 400 ℃	X_{C2H4}: 2.3% at 400 °C; X_{C2H4}: 27.72% at 615 °C; $S_{aromatics}$: 25-30% at 615 °C	X_{C2H4}: 80.8% at 400 °C; $S_{aromatics}$: 15-20% at 400 °C	-	Microwaves lower the activation energy; Microwaves activate catalytic material as well as form activated hydrocarbon intermediate
Direction conversion of ethane to ethylene [95]	4% Mo-0.5% Fe/ZSM-5; 375 ℃	X_{C2H6}: 80% and S_{C2H4}: 50% at 375 °C	X_{C2H4}: 80% and S_{C2H4}: 25% at 660 °C	Higher selectivity towards ethylene than	Presence of hot spots; Lower bulk temperature; Metal particle agglomeration;

				aromatics under MWH; Bulk reactor temperature of 375 ℃ in MWH provides the same ethane conversion as 660 ℃ in CH	
Dehydrogenation of 2-propanol [24]	Magnetite; 250 ℃	$Y_{acetome}$: 2.5% after 20 s	$Y_{acetome}$: 25% after 20 s	Inhomogeneous temperature distribution and local heating at contact points; Reaction rate under MWH corresponds	Microwave electric field gets concentrated at the contact points of spheres leading to hot spots

				to that of CH at 55 °C higher temperature	
Dehydrogenation of ethylbenzene [96]	Magnetite; 500-600 ℃	$Y_{styrene}$: 6.6% at 600 °C	$Y_{styrene}$: 23% at 600 °C	-	Microwave electric field gets concentrated at the contact points of spheres leading to hot spots
Tetralin and decalin dehydrogenation [23]	Pt/AC and Pt-Sn/AC; 250-340 ℃	$X_{tetralin}$: 86.5% at 270 °C $S_{naphalene}$>98%	$X_{tetralin}$: 98% at 270 °C $S_{naphalene}$>98 %	Lower rate of coke formation in MWH	Hot spot formation by arcing in MWH;

		$X_{decalin}$: 79.6% at 320 °C	$X_{decalin}$: 80.8% at 320 °C	compared to CH	Improvement in molecular diffusion and transport of species
		$S_{naphalene}$>80%	$S_{naphalene}$>80 %		
		$S_{tetralin}$<20%	$S_{tetralin}$<20%		

3.3 Discussion on hot spots and arcing

Formation of hot spots and arcs is a major concern during microwave heating of fluid-solid systems. Hot spots, tiny regions with much higher temperature than the surrounding, can deteriorate the reaction performance by sintering of metal particles on catalyst support [13] or producing high temperature side products, such as coke [70] that possesses excellent microwave absorbance enhancing the formation of hot spots. Experimental investigations have provided insights into the formation of hot spots and their impact on catalyst particles [13, 24]. Using X-ray diffraction and electron microscopy before and after microwave heating, significant reorganization of the catalyst was observed. For example, the formation of hexagonal crystals from amorphous metal particles dispersed over the catalyst support [13]. This reorganization has been attributed to the melting of the active metal on the catalyst support due to hot spot formation. Hot spots varied between 90 μm to 1000 μm and were at least 100-200 °C hotter than the bulk.

Hot spot formation and arcing are complex functions of size, shape, material properties, contact between particles, and electromagnetic field. The impact of the distance between

particles on hot spots and arcing was investigated by microwave heating the activated carbon particles pasted on a glass plate at varying distances [7]. Arcing is observed when the gap between the activated carbon particles is less than 9 μm, due to the concentrated electric field between particles. Arcing or electric discharge was investigated in slurries of different metal particles in organic solvents, such as benzene [9]. Metal particles concentrate the electric field at the sharp edges, and when the electric field strength surpasses the dielectric discharge strength of the solvent, arcing occurs. For metal particles and other highly conductive materials, arcing can substantially impact the reaction performance and must be accounted for. Such experiments, and even associated computations, should be extended to varying particle size, shape, and material and to a range of electromagnetic field parameters to develop a more comprehensive understanding of arcing.

In reactors with a moving solid phase, such as slurry reactors, rotation or agitation can enhance heat transfer between the phases and reduce hot spot formation and arcing [7, 12, 93]; however, hot spots can still exist even under rapid agitation [93]. In reactors with a non-movable solid phase, such as fixed beds, heat transfer is slower, and controlling hot spot formation and arcing is arduous. In such cases, structured reactors, such as monoliths and open-cell foams, can enhance heat transfer [43]. The dielectric strength of the environment can also have a significant impact on arcing. For example, the dielectric strength of sulfur hexafluoride (SF_6) and argon is three times and one-fifth, respectively, that of air (3 MV/m). Therefore, SF_6 is about an order of magnitude more resistant to arcing compared to argon. An adequate gas can be selected depending on the arcing-tendency of the microwave heated reactor.

3.4 *Summary of the experimental multiphase reactor studies: reaction selection and scale-up*

A summary of the reactions investigated along with the major observations and performance of the microwave vs. conventionally heated reactors are provided in Table 2. In most examples, microwaves enhance selectivity towards desirable products and reduce reaction time. Thus, despite the understanding of the microwave multiphase reactors being limited and the effects being mainly if not exclusively thermal, microwaves can enhance selectivity by suppressing side reactions by selective heating – whether in the gas phase or on the catalyst. Moreover, the rapid heating under microwave irradiation can significantly reduce the reaction time. To this end, controlling the temperature field during microwave heating is extremely important, especially when there is a possibility of arcing that can be detrimental to catalyst and process safety. At present, the know-how to minimize or eliminate hot spots is emerging. As such, microwave multiphase reactors provide an opportunity for reactor design and optimization.

For several catalyst materials and supports, such as ZSM-5, carbon, SiC, and alumina, the dielectric properties can change drastically at high temperatures leading to thermal runaway or cavity uncoupling, causing the material to cool [70, 105-107]. For example, the dielectric loss of SiC increases from 1.71 to 27.99 when heated from 20 ℃ and 695 ℃ [107], and the loss tangent of 7 wt% Ru/$SiTiO_3$ increases from 0.04 to 0.27 when heated from 20 ℃ to 850 ℃ [101] at 2.45 GHz. These variations occur due to changes in the physical and chemical properties, like density [80] or the mobility of charge carriers, such as electrons in SiC and cations in zeolites [70]. The dielectric properties of a material can also change due to chemical reactions. For example, coke deposition on the catalyst during methane non-oxidative coupling utilizing Mo/ZSM-5 leads to

enhanced microwave absorption ability due to the availability of delocalized π electrons in coke [70]. It is imperative to include the variation of dielectric property with temperature and progress of chemical reactions while designing microwave reactors for high temperature applications. One way to ameliorate this problem is to tune the frequency of microwave using a solid-state generator to achieve the resonant frequency for changing dielectric properties [108].

Table 2 indicates that there are several classes of reactions studied via microwaves, such as acid catalyzed chemistry of sugars, hydrogenation and oxidative dehydrogenation of hydrocarbons, emulsion polymerization, methane coupling, and the Suzuki–Miyaura cross-coupling. It would be desirable to expand this set of reactions to several other endothermic reactions. More importantly, what is missing are the underlying principles that bring out knowledge from this select set of chemistries transferable to any other chemistry given only the reaction network, the reaction rates, and the heats of reactions. These principles should inform which reactions can benefit from and how to select operating conditions along with reactor size and shape and microwave cavity and settings. Computations could in principle guide this effort to accelerate development and deployment. We propose that reactions that happen in both phases with side chemistry in one of them are ideal for microwave heating by optimizing the media and the temperature difference. For example, the non-oxidative coupling of methane over Fe/SiO_2 catalyst could lead to improved ethylene selectivity over aromatics [109].

Investigations of microwave multiphase reactors have been limited to laboratory scale size reactors of $\sim$1 cm^3. Table 3 summarizes the size of multiphase systems studied under microwave irradiation. Deployment of microwave reactors in chemical industry would require their scale-up, i.e., going from lab-scale to industrial-scale. Non-uniformity of the temperature field and limited

penetration of microwaves will be major challenges during scale-up. Yet, this is doable. Santamaria and co-workers demonstrated 150× increase in the reactor volume for methane non-oxidative coupling [70] and methane dehydroaromatization [108]. Significant steps required to achieve this scale-up were using 915 MHz frequency, allowing higher penetration depth and larger waveguide and cavity, and rotating the reactor to maintain a uniform temperature similar to the use of a turntable in a kitchen microwave oven. A waveguide, hollow metallic tube, is commonly used during scale-up as it can deliver a higher power at a lower cost than coaxial cables. Interestingly, the energy efficiency was much higher for the scaled-up version; microwave power was increased by 6× for a 150× increase in the reactor size pointing to the nonlinear relationship between power and temperature [108]. This behavior was qualitatively predicted by our recent simulations [40]. Although application of microwave reactors in chemical industry is scare, a few pilot-scale demonstrations exist. For example, a microwave-assisted exhaust gas treatment setup with 4 KW input power [110]. Such investigations are needed for processes with success at the lab-scale.

In industrial applications, multimode applicators are used with tunnel-like microwave cavity combined with conveyer belts, enabling a continuous operation. At present, single-mode or mono-mode microwave cavities, maintaining a uniform microwave field intensity, are used at the lab-scale. Maintaining a uniform field at a large scale is challenging using the current technology. Innovation in microwave cavity design is imperative to overcome these hurdles. One such example is the *traveling microwave reactor* based on a coaxial cable to allow a uniform microwave field for continuous flow reactors [47].

We end this subsection with a brief discussion on solid-state generators that generate high precision microwaves utilizing transistors. In contrast to magnetrons, a single frequency from a range can be produced precisely. For example, a 915 MHz solid-state generator can produce microwaves with a single frequency in the range of 902 to 928 MHz [108]. Coupled with a commercially available auto-tuning software, a solid-state generator can be operated at the resonant frequency providing excellent coupling with materials with changing dielectric properties. Moreover, the lifespan of solid-state generators is much longer (∼20 years) compared to magnetrons (∼1000s hours) [63]. Two major hurdles limit the widespread use of these generators: high cost and limited power output (< 1KW). For this reason, industrial installations commonly use magnetrons that are cheaper and can provide high power output (< 1 MW) [63]. Current trends indicate decreasing cost and increasing power output of solid-state generators. In the future, the solid-state generators are expected to play an essential role in microwave heating applications.

Table 3: Size of different multiphase reactors investigated in the literature.

Reactor Type	Reactor Size Range	Input power range [W]	References
Liquid-in-Liquid/Emulsion	Volume: 45-250 mL	65-1000	[26, 88, 91, 92, 111, 112]
Biphasic	Volume: 5-100 mL	20-200	[72, 92, 104, 111]
Monolith	Diameter: 12-37 mm	20-700	[5, 19-22, 102]

	Length: 12-20 mm		
Slurry	Diameter: 11-25 mm Length: 16-185 mm	50-1000	[7, 10-12, 14]
Fixed Bed	Diameter: 5-24 mm Length: 19-20 mm	5-320	[15, 16, 23, 24, 32, 96]

4. Modeling of microwave heated reactors

The governing equations and the boundary conditions for microwave heating of a multiphase reactor are provided in Appendix A. These equations along with appropriate boundary conditions can be solved to predict microwave heating of single and multiphase systems. All the governing equations along with the appropriate boundary conditions are coupled and solved simultaneously using a finite volume or finite element-based method often employing a commercial software, such as COMSOL [113]. The multiscale nature of the problem makes the problem stiff by introducing a large separation of length and time scales. For example, the length scale varies from the size of a solid particle or a liquid droplet to the entire reactor. For accurate numerical solution, the mesh or element size needs to be sufficiently smaller than the smallest scale present, making the computational cost of the simulations extremely high.

The CPU cost and memory requirement are proportional to the number of mesh elements; there is often a quadratic or higher dependence of the CPU cost on the number of mesh elements

depending on the numerical method employed. Figure 5a illustrates the mesh for a single unit cell, i.e., the smallest periodic structure whose replication creates an entire material, of a multiphase system consisting of dispersed and continuum phases, resolving the dispersed phase. An estimate of the number of mesh elements required for fully resolved three-dimensional simulations of various lab-scale multiphase systems is shown in Figure 5b. Simulations of fixed beds are the most expensive, followed by monoliths and slurries. The computational cost of multiphase systems can be three to five orders of magnitude higher than that of single-phase and biphasic systems. Therefore, fully resolved simulations of even lab-scale multiphase reactors is prohibitive. Due to this reason, most simulations of microwave heating either focus on single-phase systems or oversimplify multiphase systems. The next subsection reviews the simulation investigations of microwave heating of multiphase systems.

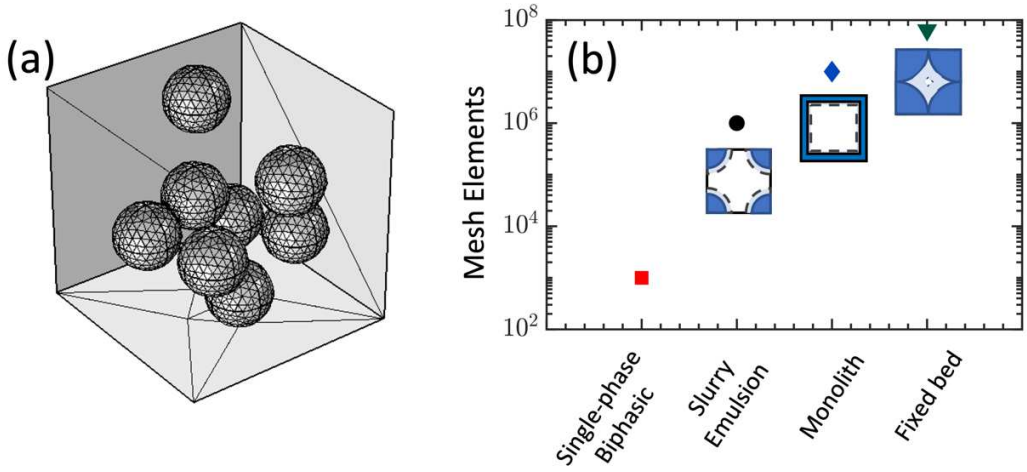

Figure 7: (a) Meshing of a unit cell of a multiphase system. For detailed simulations, the mesh needs to resolve the smallest scales present in a multiphase system, i.e., of the dispersed phase. (b) Illustrative estimate of required number of mesh elements for various three-dimensional multiphase reactors: single-phase and biphasic systems (red square), slurry and emulsion (black sphere), monolith (blue diamond), and

fixed bed (green inverted triangle). In the calculations, the separation of length scale, ratio of the largest to the smallest length scale, is set to ten representing a reactor of dimension 1 cm and the smallest scale of 1 mm. In fixed beds, resolving the particles and the contact points between them require mesh elements smaller than $d_p/40$ [114]. For a slurry/emulsion and monoliths, ten mesh elements are used to resolve the smallest features, which are the particle and the wall thickness in a slurry/emulsion and monolith, respectively. For each reactor dimension, at least ten mesh elements are used.

4.1 *Microwave heating using simplified approaches*

There is limited number of modeling and simulation studies of microwave multiphase reactors and most of them focus on non-reacting cases and fixed beds. The multiphase system is typically treated as a continuum using an experimentally measured effective permittivity [45, 96] to overcome the multiphase and multiscale nature of the problem, whereas other physical properties, like the thermal conductivity, are either based on the volume fraction of each phase or tuned to get a better match with the experiments [96]. The effective properties, such as the thermal conductivity, based on volume fraction may not be accurate, especially when the properties of different materials vary significantly. In such cases, numerical homogenization can provide an accurate estimate of the effective properties [115]. In cases where the continuum assumption is not made, only a single particle is modeled [24] that makes comparison with experiments unreliable. Most of these studies do not report grid independence, which is important for particle-resolved simulations. Comparison with experiments has been reported in a few cases only [96].

In [96] microwave heated dehydrogenation of ethylbenzene over magnetite catalyst particles in a fixed bed (bed diameter: 8 mm and height: 20 mm) was simulated using the continuum

approximation with effective properties. The effective permittivity was measured experimentally, whereas the effective thermal conductivity was tuned along with the microwave power to obtain a good fit between the simulation and experimental bed temperature. Given the fitted parameters on the one hand and the limited spatial information on the other, rigorous assessment of the model is infeasible. Microwave heating of a C/SiO_2 aerogel filled with hydrides was simulated [45] assuming the aerogel to be a continuum using the experimentally measured permittivity. Even though the electromagnetic field distribution was highly non-uniform, the temperature distribution was uniform due to the high thermal conductivity. In both studies [45, 96], mesh independence study was not reported.

Apart from continuum assumption, a few studies have modeled a single particle surrounded by a fluid [6, 116]. Wang et al. [116] modeled the heating of a silicon carbide particle surrounded by paraffin oil in a two-dimensional geometry. The absorbed microwave power by the silicon carbide was indirectly estimated using the experimentally measured temperature rise of the paraffin oil, with and without silicon carbide. The temperature difference between the particle and the surrounding liquid was proportional to the heating time due to the assumption of a constant heat transfer rate between the two phases. However, the heat transfer rate between the two phases should be proportional to their temperature difference. We have recently shown that the temperature difference T_D between the two phases (in a slurry) varies as $T_{D,\max}\left(1 - e^{-t/\tau}\right)$, where $T_{D,\max}$ is the maximum value of T_D achieved at times much longer than the characteristic time scale τ of the system [67]. Simulations of microwave heating of a gas bubble surrounded by a liquid have also been performed [6]. These simulations showed that a sharp variation in dielectric properties across the gas-liquid interface leads to a significantly

distorted electric field around the bubble causing rapid heating of the liquid near the bubble interface.

Resolved simulations of a fixed bed [24] and a monolith [43] have recently been performed. In [24], the experimental setup included a fixed bed of magnetite particles with a diameter of around 400 μm arranged randomly. However, the simulation setup considered particles of diameter 1.9 mm in a cubic lattice (Figure 8), i.e., the number of particles is fewer than the experiments by 100×. Due to this assumption the number of particles in the simulation are lesser by a factor of 100 compared to the experiments. When particles are in contact, grid refinement becomes critical; however, grid independence was not reported. Despite these limitations, the simulation provided excellent agreement with a few temperature measurements made using fiber optics. The simulations revealed extremely high electromagnetic power loss density at the contact points (see Figure 8d) leading to higher temperature at the contact point compared to the bulk.

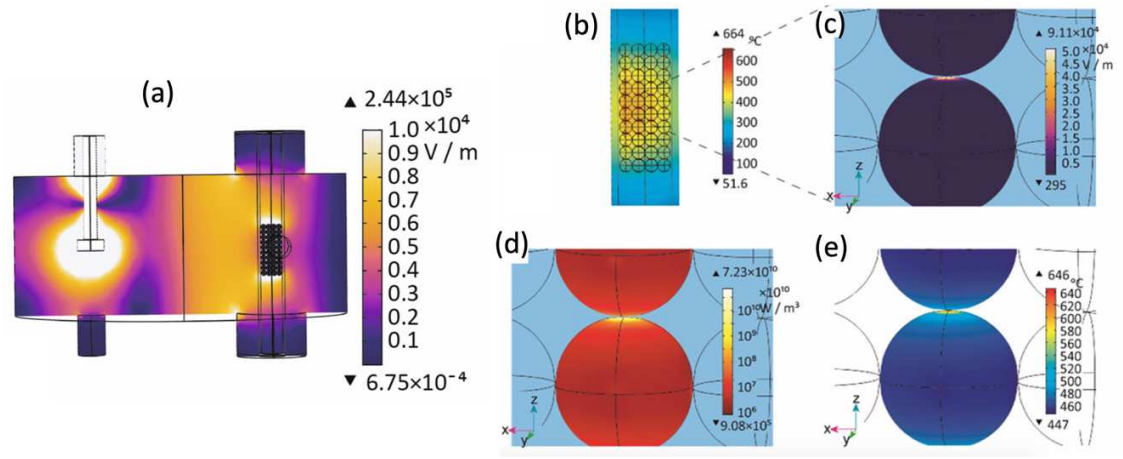

Figure 8: Particle-resolved simulation for a fixed bed. (a) Microwave cavity along with the fixed bed; (b) A two-dimensional cross section of the fixed bed showing the temperature distribution; (c), (d), and (e)

electric field strength, volumetric energy dissipation, and temperature distribution near the contact point of two particles. (Reprinted with permission from the publisher; Haneishi et al. [24]).

In the resolved simulations of a monolith [43], computational fluid dynamics (CFD) simulations coupled with electromagnetic field solver were performed using COMSOL. The computational geometry along with the cross-sectional temperature profiles are shown in Figure 9a and b, respectively. These simulations predict the temperature of monolith walls and the fluid flowing through the monolith channels for various materials and flow conditions. The predictions of the spatial temperature profile agree well with the IR thermal camera data and thermocouples outside the bed (shown in Figure 9c). Furthermore, this work demonstrates that the temperature gradient between the monolith walls and the fluid depends on the fluid residence time and transverse heat transfer time scale. Such computations can be used to maximize or minimize the temperature gradient for a given application.

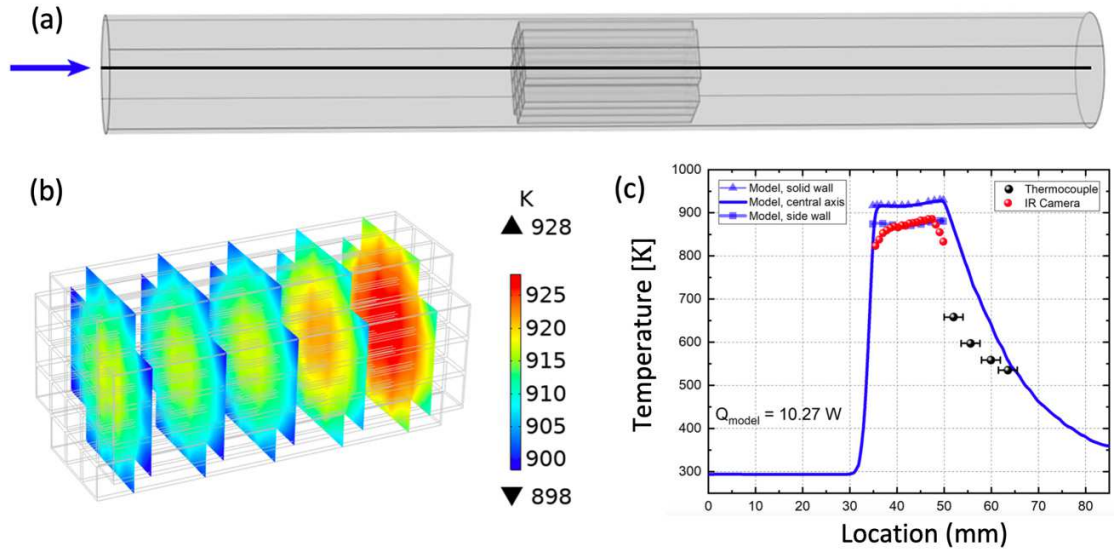

Figure 9. (a) Computational setup for microwave heating of monolith in a quartz tube with air flow of 100 SCCM from left. (b) Cross-sectional color maps of temperature in the monolith at z=1.5, 4.5, 7.5, 10.5,

and 13.5 mm from the monolith inlet. (c) The blue triangles denote the predicted temperature of the solid wall around the central channel, and blue squares are the temperatures of the outer edge of the side channel. The red and black points show the temperatures measured using an IR camera and thermocouple, respectively. Error bars account for the thermocouple placement error (± 2 mm) downstream from the monolith. (Reprinted with permission from the publisher; Malhotra et al. [43]*).*

Modeling studies of microwave heating of other fluid-solid reactors, such as fluidized beds [117, 118] are scarce; most of these studies are rather simplistic. For example, in [119] CFD simulations of microwave heating of lignite in a fluidized bed was performed using the Euler-Euler strategy for the bed hydrodynamics. A simplistic expression for the microwave power absorbed was used instead of solving the Maxwell's or Helmholtz equations. Most of the microwave heating simulations reported here utilize COMSOL. Only a few studies are based on other software, such as ANSYS [120] and OpenFOAM [121].

In summary, it is imperative to develop adequate models that are validated against experiments to aid understanding the experimental observations and to design and optimize novel intensified microwave multiphase reactors. The reported simulations either employ a continuum approximation requiring the experimentally measured effective properties, such as permittivity and conductivity, or use a small number of particles to reduce the computational cost. Spatially resolved experimental measurements have been by and large lacking. Thus, validation of models has been limited and models have been mostly fitted rather than been interpretive or even better predictive. Such reductionistic approach cannot be employed for understanding and optimizing multiphase reactors. Moreover, the energy dissipation and temperature in each phase cannot be inferred. The need to simplify modeling of multiphase

systems stems from the exorbitant computational cost associated with their multiscale and multiphase nature. To tackle this challenge, high-fidelity and computationally affordable multiscale modeling approaches are needed.

4.2 *Multiscale modeling*

Multiscale first-principles modelling is necessary to make high-fidelity predictions and handle the computational cost associated with the large separation of scales. For the energy, momentum, mass, and species conservation equations several multiscale methodologies exist. Examples include representing a fixed bed as a porous medium [122], using the Euler-Lagrange [123, 124] or the Euler-Euler [125] approach for a slurry or a fluidized bed. Depending on the size of the multiphase system and the details required, an appropriate model can be selected. Even though several techniques exist for conventional heating of multiphase systems, such methodologies are uncommon for microwave heating.

Homogenization or coarse-graining is a technique that has successfully been implemented for multiscale problems, such as species diffusion [126-128] and thermal conduction [129, 130]. Homogenization theory takes advantage of the disparity in length scales and provides effective properties, thereby converting the original point-wise mathematical description into an averaged (coarse-grained) description. Figure 10 shows a schematic of the homogenization methodology. Detailed simulations at the unit cell level, i.e., the smallest periodic structure whose replication creates an entire system, are performed to evaluate the effective properties of the pseudo homogeneous or effective medium. The advantage of the homogenization theory is that it can be applied to periodic and non-periodic structures alike. In the latter case, the unit cell must be

large enough to capture the statistical distribution of the constituent materials and microstructure.

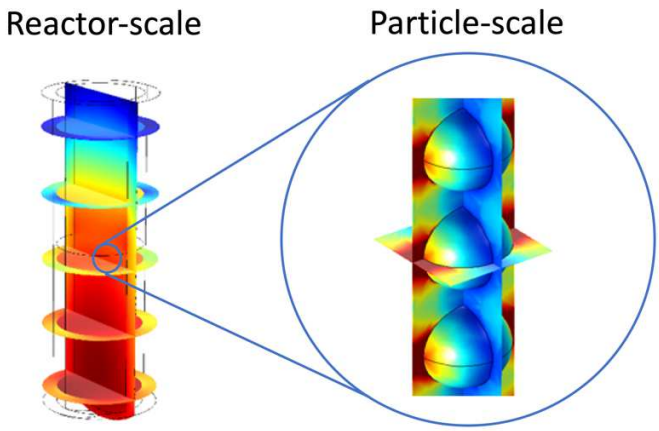

Figure 10: Schematic of the homogenization/coarse-graining approach. At the reactor scale, a multiphase system is represented by a homogeneous or effective medium. The properties of the effective medium are calculated based on detailed simulations in a unit cell of the multiphase system.

Recently, we have developed a methodology based on homogenization for microwave-heated multiphase systems leading to a significant reduction in the computational cost while retaining the accuracy of the computationally expensive detailed simulations [131]. We have assessed the methodology with detailed particle-resolved simulations [131] and experiments of microwave heated slurries [67]. In our methodology, the length scales of the multiphase system and the unit cell are defined as $\mathcal{L}_c$ and l_c, respectively, such that $l_c \ll \mathcal{L}_c$. Figure 11 shows the schematic of a multiphase system (e.g., a fixed bed or a slurry reactor) along with the associated length scales.

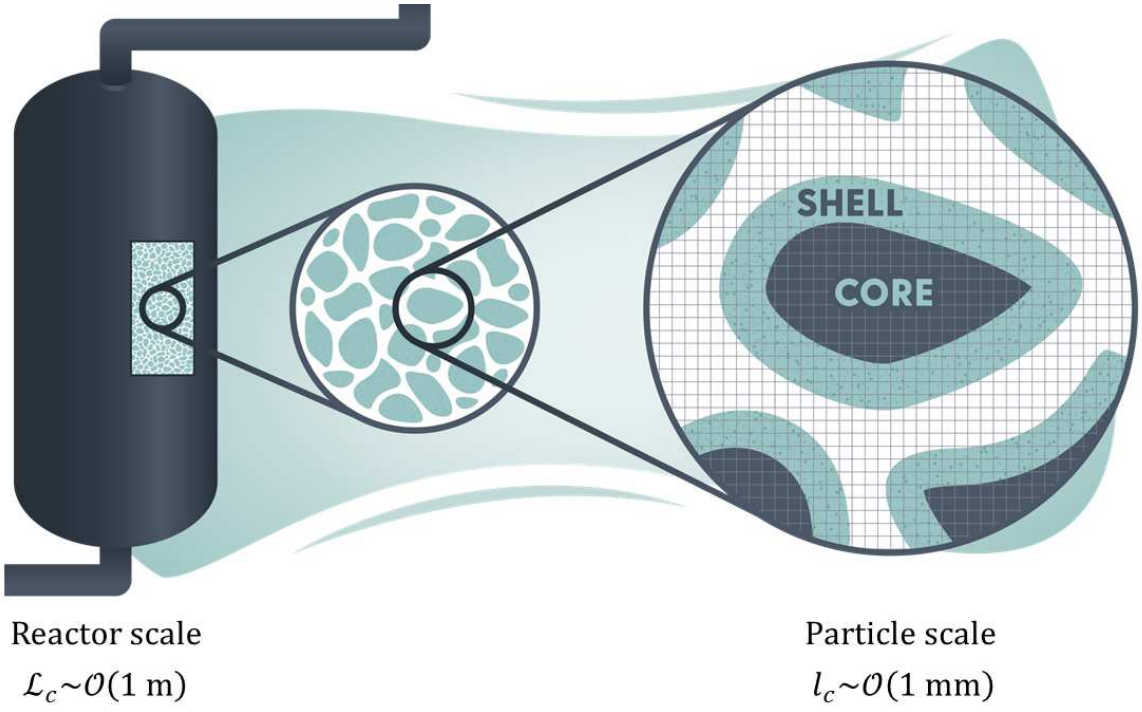

Figure 11. Schematic of the multiscale nature of a multiphase catalytic reactor. The largest length scale corresponds to the reactor-size $\sim\mathcal{O}(1\ m)$ and the smallest length scale is associated with a single particle $\sim\mathcal{O}(1\ mm)$. In detailed simulations, the mesh size needs to be sufficiently smaller than the particle size, making the number of mesh elements too large to be computationally affordable. (Reprinted with permission from the publisher; Goyal and Vlachos [131]*).*

To obtain the governing equations for the effective medium, the averaging operator $\langle\cdot\rangle$ is defined over the length scale l_c as:

$$\langle\cdot\rangle = \frac{1}{\mathcal{V}}\int_{\mathcal{V}} (\cdot)dV \qquad (1)$$

where $\mathcal{V}$ is the volume associated with the length scale l_c. The effective permittivity $\varepsilon_{\mathrm{eff}}$ and the effective thermal conductivity κ_{eff} can be calculated as:

$$\varepsilon_{\text{eff}} = \frac{\langle D \rangle}{\langle E \rangle} \tag{2}$$

$$\kappa_{\text{eff}} = \int_0^1 \int_0^1 \int_0^1 \kappa(x_1, x_2, x_3) \frac{\partial T}{\partial x_1} dx_1 dx_2 dx_3 \tag{3}$$

Here, $\langle D \rangle$ and $\langle E \rangle$ are the electric displacement field D and the electric field E averaged over the unit cell of a multiphase system. κ and T are the space-dependent thermal conductivity and temperature, and $x_1, x_2, \text{and } x_3$ are the spatial coordinates. The power absorbed in the solid phase $\langle Q \rangle_{\text{s}}$, the fluid phase $\langle Q \rangle_{\text{f}}$, and the overall multiphase system $\langle Q \rangle_t$ is calculated as:

$$\begin{aligned} \langle Q \rangle_{\text{s}} &= 0.5\omega\varepsilon_{\text{s}}''\beta(1+\alpha)\langle E \rangle.\langle E^* \rangle \\ \langle Q \rangle_{\text{f}} &= 0.5\omega\varepsilon_{\text{f}}''\frac{(1-\phi\beta)}{(1-\phi)}(1+\alpha)\langle E \rangle.\langle E^* \rangle \\ \langle Q \rangle_t &= \phi\langle Q \rangle_{\text{s}} + (1-\phi)\langle Q \rangle_{\text{f}} \end{aligned} \tag{4}$$

where ϕ is the solid volume fraction, E^* is the complex conjugate of E, and ε_{s}'' and ε_{f}'' are the imaginary part of the relative permittivity of the solid and fluid phases, respectively. α and β capture the variation of E within the unit cell and are calculated using the numerically evaluated E within the unit cell:

$$\begin{aligned} \alpha &= \frac{\langle E'.E'^* \rangle}{\langle E \rangle.\langle E^* \rangle} \\ \beta &= \frac{\langle E.E^* \rangle_{\text{s}}}{\langle E.E^* \rangle} \end{aligned} \tag{5}$$

Here, $\langle \cdot \rangle_s$ is the averaging operator defined over the solid phase in the unit cell. More details about the multiscale methodology and the calculation of the effective properties can be found in [131].

The effective electromagnetic properties, such as permittivity and permeability, can be calculated once at the beginning of the simulation based on the unit cell calculations. If the electromagnetic properties are sensitive to temperature, then the effective properties need to be computed for a range of temperature. In the general case of a dynamic multiphase reactor, such as a slurry and a fluidized bed, the effective properties also need to be calculated for a range of the dispersed phase volume fractions, using CFD simulations. In this manner, the multiscale methodology for Maxwell's or Helmholtz equations can be coupled with the well-known multiscale methodologies for the transport equations. Figure 12 shows a schematic for how different multiscale approaches for the transport equations can be coupled with the homogenized electromagnetic field equations.

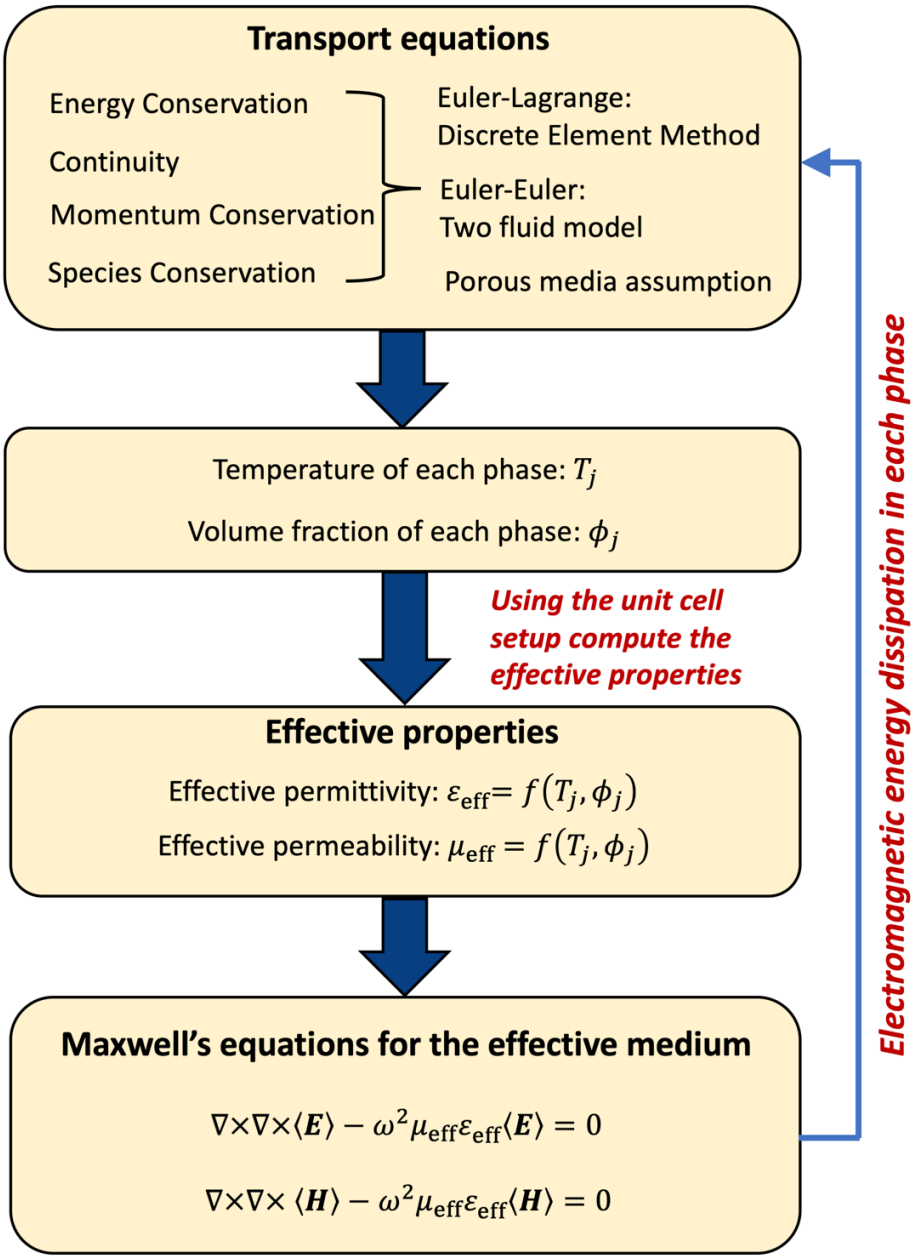

Figure 12: Schematic depicting the coupling of the homogenized/coarse-grained equations for the electromagnetic field with the conservation equations for continuity, energy, momentum, and species.

One limitation of homogenizing the temperature field is the loss of temperature profile within a unit cell, which can have a significant impact on temperature-sensitive catalytic reactions. The

temperature variation within the unit cell level on catalytic reactions must be assessed. In our recent work [131], we introduced a simple time-scale analysis to estimate the critical unit cell size l_c^* above which temperature variations are significant (> 10 K):

$$l_c^* = \sqrt{\frac{10\alpha}{\Delta \dot{T}_{\max}}} \tag{6}$$

where, α is the effective thermal diffusivity of the material in the unit cell and $\Delta \dot{T}_{\max}$ is the maximum difference in the rate of temperature increase between two points within the unit cell. In essence, Eq. (6) evaluates the rate for energy diffusion across the unit cell relative to the rate of energy input. Figure 13 shows the simulated intra-particle temperature profiles after five seconds of microwave-heating. The temperature non-uniformity within the unit cell is significant ($\sim$10 K) when $l_c > l_c^*$, and negligible when $l_c < l_c^*$. These results are independent of the dielectric properties of the constituent materials. Using Eq. (6), the temperature variation at the particle-scale can be evaluated before applying homogenization to assess if the unit cell can be assumed to be isothermal or one must resolve and use the gradients within it.

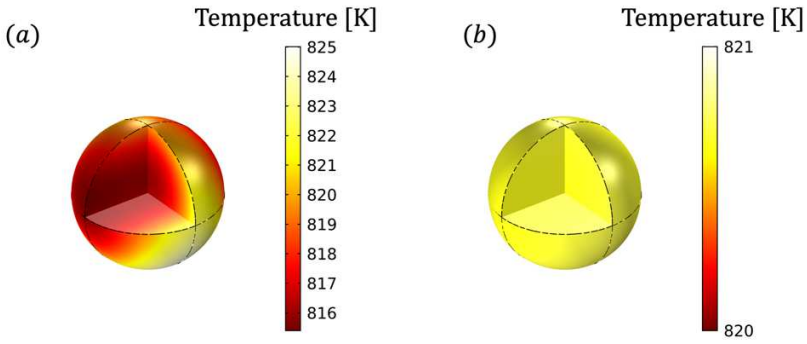

Figure 13. Intra-particle temperature profiles obtained from the simulations of microwave-heating of spherical particles of diameter 1 mm with solid volume fraction set to 0.25. (a) $l_c > l_c^*$, (b) $l_c < l_c^*$. (Reprinted with permission from the publisher; Goyal and Vlachos [131]*).*

At present, multiscale modeling of microwave heated multiphase reactors is in its infancy. Our initial success [67, 131] shows that further work in this direction could lead to reliable and computationally affordable computational tools. These tools are needed to quantify the vast experimental data that has rapidly increased.

5. Conclusions and outlook

Numerous investigations have demonstrated process intensification of microwave heating manifested with higher product yield and selectivity, reduced coke and catalyst deactivation, reduced processing time, and higher energy efficiency. However, demonstration of improved performance with microwave heating is currently limited to a case-by-case situation. Transferable knowledge that can be applied to any endothermic reaction prior to conducting experiments is missing but imperative to guide experimentation. Most of the investigations ascribe microwaves' ability to achieve process intensification to the selective heating that causes temperature gradient between phases. This temperature gradient can change reactor performance by, for example, localizing reactions in one phase and minimizing side reactions in the other. Although controversial, some studies attribute the improved performance under microwave irradiation to a reduced activation energy (non-thermal effect). However, these studies do not provide quantitative prediction or measurement of the temperature field in the reactor. Given temperature differences between phases and the potential non-uniform temperature field in a reactor, non-thermal microwave effects need to be supported by detailed temperature evaluation.

The confusion in the community regarding the mechanism of microwave-assisted process intensification stems from the great difficulty in accurate measurement of temperature in a microwave multiphase reactor. Preliminary success in this direction has been made in monoliths, where temperature measurement of both solid and gas phases is made during microwave heating. These measurements have supported a picture whereby the lower temperature of the gas phase is responsible for the performance enhancement due to reduced side reactions. Such spatially resolved techniques and measurements are missing for other multiphase reactors and should be the focus of future studies if the field were to be significantly advanced.

Selective heating in microwave multiphase reactors can lead to hot spots and arcing that can either enhance or reduce reactor performance. Hot spots are linked to sintering of metal nanoparticles on a catalyst support, thereby reducing catalyst activity, and could cause material failure if the maximum temperature exceeds materials specifications. However, hot spots can enhance desorption and the rate of mass transfer away from the catalyst surface, leading to reduced catalyst deactivation. Detailed investigations are needed for better understanding of the formation and role of hot spots in reaction performance. In addition, criteria for their elimination whenever are undesirable should be developed. Structured reactors, such as monoliths, of conductive materials as well as fast flow and mixing could be designed and utilized for effective energy dissipation and hot spot elimination. The introduction of micro fixed bed monoliths provides versatility in material, high catalyst loading, uniform temperature, and hot spot elimination.

The challenges before microwave multiphase reactors make predictive computational tools desirable. Progress in the simulations of multiphase microwave reactors has been hindered by

the multiscale nature of the problem, requiring a computational cost of three to five orders of magnitude higher than of a single-phase system. This exorbitant computational cost necessitates major model simplifications compromising the accuracy of the simulations and the comparison to experiments. Multiscale modeling, such as homogenization and coarse graining more generally, has the potential to significantly reduce the computational cost while maintaining simulation accuracy. Such computational tools could enable computational optimization and scale-up of microwave-assisted processes in chemical industry. We believe this is entirely doable but requires advances in modeling and simulation, along with measurements of thermophysical and materials properties and accurate kinetics.

Future studies on less explored microwave multiphase reactors are expected to reveal new physics and opportunities to redesign chemical processes to achieve further process intensification. A key fundamental problem for future work is the prediction of the temperature difference between phases so one can purposely design reactors to increase or decrease this difference. Scale-up studies and additive manufacturing offer new opportunities for realizing multiphase reactors. Developing design principles for selecting chemical reactions, media, and operating conditions is much needed.

Appendix: Governing equations

Chemical transformations in a multiphase microwave reactor are modeled by the governing equations for electromagnetic field coupled with the governing equations of mass, momentum, continuity, and energy conservation. Maxwell's equations describe the distribution of electromagnetic field given by:

$$\nabla \times \bar{E} = -\frac{\partial \bar{B}}{\partial t}$$

$$\nabla \times \bar{H} = \frac{\partial \bar{D}}{\partial t} + \bar{J} \qquad \text{(A1)}$$

$$\nabla . \bar{D} = \rho_q$$

$$\nabla . \bar{B} = 0$$

where, $\bar{E}$ is the electric field in V/m, $\bar{H}$ is the magnetic field in A/m, $\bar{D}$ is the electric flux density in C/m^2, $\bar{B}$ is the magnetic flux density in Wb/m^2, $\bar{J}$ is the electric current density in A/m^2, and ρ_q is the electric charge density in C/m^3. The above equations are valid for any time-dependent electric and magnetic fields. For an electromagnetic wave with sinusoidal or harmonic time-dependence (e.g., microwaves), usage of phasor notation becomes convenient. In the phasor notation, $e^{j\omega t}$ time-dependence is assumed for all the field quantities. For example,

$$\bar{E}(\mathbf{r}, \mathrm{t}) = \mathrm{Re}\left[E(\mathbf{r})e^{j\omega t}\right]$$

where E is the amplitude of the wave and $\mathrm{Re}(\cdot)$ is the real value of a quantity $(\cdot)$. $e^{j\omega t}$ is dropped from the field quantities and Maxwell's equations, in the phasor form, can be written as:

$$\nabla \times E = -j\omega B$$

$$\nabla \times H = j\omega D + J \qquad \text{(A2)}$$

$$\nabla . D = \rho_q$$

$$\nabla . B = 0$$

In a linear medium, i.e., ε and μ are independent of E and H, B is related to H, and D and J are related to E through the constitutive relations:

$$D = \varepsilon E$$

$$B = \mu H \qquad \text{(A3)}$$

$$J = \sigma E$$

where, ε, μ, and σ are the complex permittivity, permeability, and electric conductivity of a material that are a function of the angular frequency ω and the temperature. In a general anisotropic medium, ε and μ are tensors of rank two. Assuming the medium to be isotropic, ε and μ become scalars. The imaginary part of ε and μ accounts for the loss due to the damping of the vibrational or translational motion of the dipoles or ions/electrons caused by electromagnetic waves. Using the constitutive relations, Maxwell's equations in phasor form in a linear and isotropic medium become:

$$\nabla \times E = -j\omega\mu H$$

$$\nabla \times H = j\omega\varepsilon E + \sigma E \qquad \text{(A4)}$$

$$\nabla.(\varepsilon E) = \rho_q$$

$$\nabla.(\mu H) = 0$$

Further assuming that the medium is homogeneous and by taking the curl of the first two equations, separate equations can be obtained for E and H known as Helmholtz or wave equations, given by:

$$\nabla \times \nabla \times E - k^2 E = 0$$

$$\nabla \times \nabla \times H - k^2 H = 0 \qquad \text{(A5)}$$

Here, $k = \omega\sqrt{\mu\varepsilon^*}$ is the propagation constant and $\varepsilon^* = \left(\varepsilon - j\frac{\sigma}{\omega}\right)$. It should be noted that when the permittivity is measured experimentally using the perturbation technique, it includes the effect of electric conductivity. In those cases, the electric conductivity should be set to zero

in the computations [96]. Upon further assuming that the medium is source-free or free of charge, i.e., $\rho_q = 0$, Helmholtz equations can be simplified to obtain:

$$\begin{aligned} \nabla^2 E + k^2 E &= 0 \\ \nabla^2 H + k^2 H &= 0 \end{aligned} \tag{A6}$$

It is convenient to use the relative permittivity, $\varepsilon_r = \varepsilon/\varepsilon_0 = \varepsilon' - j\,\varepsilon''$, and the relative permeability, $\mu_r = \mu/\mu_0 = \mu' - j\mu''$, with $\varepsilon_0 = 8.854 \times 10^{-12}$ F/m and $\mu_0 = 4\pi \times 10^{-7}$ H/m being the permittivity and permeability of the free space, respectively. ε' quantifies the ability of the material to store the electrical energy, whereas ε'' describes the material's ability to dissipate the stored electrical energy into heat. At a physical level, ε' is related to the material's ability to create dipoles, ions, and free electrons, whereas ε'' is related to the resistance experienced during the motion of the charged entities by the oscillating microwaves. μ' and μ'' are analogous to ε' and ε'' for the magnetic field component of an electromagnetic wave. Another important quantity is the electric $\tan\delta_e$ and magnetic loss tangent $\tan\delta_m$ defined as:

$$\begin{aligned} \tan\delta_e &= \frac{\varepsilon''}{\varepsilon'} \\ \tan\delta_m &= \frac{\mu''}{\mu'}. \end{aligned} \tag{A7}$$

$\tan\delta_e$ and $\tan\delta_m$ quantify the ability of a material to be heated in an electromagnetic field. Higher values of $\tan\delta_e$ and $\tan\delta_m$ are associated with a higher propensity toward microwave heating.

The tangential components of the electric and magnetic fields are continuous across an interface between two mediums with no charge or surface current density and can be written as:

$$\hat{n} \times E_1 = \hat{n} \times E_2$$
$$\hat{n} \times H_1 = \hat{n} \times H_2 \quad \text{(A8)}$$

where $\hat{n}$ is the unit normal vector at the interface between medium 1 and 2. $E_1$and E_2 are the electric fields in medium 1 and 2, respectively, and H_1 and H_2 are the magnetic fields in medium 1 and 2, respectively. We suggest the textbook by Pozar [60] for more details on the mathematical background of the governing equations of an electromagnetic field.

In the literature, as a simplification, Lambert's law is sometimes used for the distribution of microwave power in a material, given by

$$P(r) = P_0 e^{-2\beta r} \quad \text{(A9)}$$

where, P_0 is the transmitted power flux into the medium and $P(r)$ is the power flux at a distance r from the sample surface. β is the attenuation constant that controls the rate of decay of the incident electromagnetic power and is defined as the imaginary part of the propagation constant k:

$$\beta = \frac{\omega}{c}\left[\frac{\varepsilon'\left(\sqrt{1+\tan^2\delta}-1\right)}{2}\right]^{\frac{1}{2}} \quad \text{(A10)}$$

where, c is the speed of light. The half of inverse of β is known as the penetration depth l_p, which is the distance at which the intensity of an electromagnetic wave decreases to $1/e$ of its incident value [132]:

$$l_p = \frac{1}{2\beta} = \frac{c}{2\omega}\left[\frac{2}{\varepsilon'\left(\sqrt{1+\tan^2\delta}-1\right)}\right]^{\frac{1}{2}} \quad \text{(A11)}$$

Lambert's law is only valid in the limit of semi-infinite sample thickness and does not account for the standing wave effect [51]. Therefore, in most of the lab-scale microwave reactors,

Lambert's law cannot be used, and the governing equations of electromagnetic waves need to be solved to obtain the distribution of electromagnetic energy dissipation.

The temperature profile of the medium being heated in a microwave field can be evaluated by solving the energy conservation equation:

$$\rho C_p \frac{\partial T}{\partial t} + \rho C_p \boldsymbol{u}.\nabla T = -\nabla.(\kappa \nabla T) + Q_p \qquad \text{(A12)}$$

where ρ, C_p, and κ are the mass density, specific heat capacity, and thermal conductivity of the medium, respectively. T and $\boldsymbol{u}$ are the temperature and fluid velocity at a given point inside the medium. An adiabatic boundary condition is used at the outside boundary of the reactor if insulation is used, otherwise heat losses due to convection and radiation are imposed. At the interface of two mediums, thermal equilibrium is assumed. The volumetric power absorbed Q_p in the medium due to the electromagnetic energy dissipation caused by the conduction loss, dielectric heating, and magnetic heating is given by:

$$Q_p = \frac{1}{2}\sigma|E|^2 + \frac{1}{2}\omega\varepsilon_0\varepsilon''|E|^2 + \frac{1}{2}\omega\mu_0\mu''|H|^2 \qquad \text{(A13)}$$

where $|E|$ and $|H|$ represent the magnitude of E and H, respectively. The equations for electromagnetic field are directly coupled to the energy conservation equation due to the temperature dependence of the electrical conductivity, permittivity, and permeability. A change in these electromagnetic properties modifies the electromagnetic field distribution inside the reactor cavity, which in turn affects the energy dissipation and the temperature within the material. Therefore, the knowledge of how these properties vary with temperature is imperative.

For the velocity field of the continuum phase, the Navier-Stokes and the continuity equations need to be solved. For a dynamic dispersed phase, two common techniques utilized are the

Eulerian approach [125], where the dispersed phase is assumed to be a continuum, and the Lagrangian approach [123, 124], where individual particles are tracked. In the case where one phase is stationary, such as the solid phase of a monolith, the velocity distribution of the fluid phase is only required. In a reacting system, the species conservation equations also need to be solved to obtain species concentrations.

Acknowledgements

This work was supported in part by the Indian Institute of Technology Madras Seed Grant, award number CH1920829NFSC008954 and the RAPID manufacturing institute, supported by the Department of Energy (DOE), award number DE-EE0007888-8.3. The Delaware Energy Institute is grateful to the State of Delaware for its support of the RAPID institute projects.

References

[1] J. Newman, C. A. Bonino, and J. A. Trainham, "The energy future," *Annual review of chemical and biomolecular engineering,* vol. 9, pp. 153-174, 2018.

[2] D. A. Jones, T. P. Lelyveld, S. D. Mavrofidis, S. W. Kingman, and N. J. Miles, "Microwave heating applications in environmental engineering—a review," *Resources, conservation and recycling,* vol. 34, no. 2, pp. 75-90, 2002.

[3] J. Hu *et al.*, "Microwave-driven heterogeneous catalysis for activation of dinitrogen to ammonia under atmospheric pressure," *Chemical Engineering Journal,* p. 125388, 2020.

[4] R. Luque, J. A. Menendez, A. Arenillas, and J. Cot, "Microwave-assisted pyrolysis of biomass feedstocks: the way forward?," *Energy & Environmental Science,* vol. 5, no. 2, pp. 5481-5488, 2012.

[5] I. Julian, H. Ramirez, J. L. Hueso, R. Mallada, and J. Santamaria, "Non-oxidative methane conversion in microwave-assisted structured reactors," *Chemical Engineering Journal,* vol. 377, p. 119764, 2019.

[6] M. De Bruyn *et al.*, "Subtle microwave-induced overheating effects in an industrial demethylation reaction and their direct use in the development of an innovative microwave reactor," *Journal of the American Chemical Society,* vol. 139, no. 15, pp. 5431-5436, 2017.

[7] S. Horikoshi, A. Osawa, S. Sakamoto, and N. Serpone, "Control of microwave-generated hot spots. Part V. Mechanisms of hot-spot generation and aggregation of catalyst in a microwave-assisted reaction in toluene catalyzed by Pd-loaded AC particulates," *Applied Catalysis A: General,* vol. 460, pp. 52-60, 2013.

[8] T. D. Musho, C. Wildfire, N. M. Houlihan, E. M. Sabolsky, and D. Shekhawat, "Study of Cu2O particle morphology on microwave field enhancement," *Materials Chemistry and Physics,* vol. 216, pp. 278-284, 2018.

[9] W. Chen, B. Gutmann, and C. O. Kappe, "Characterization of Microwave-Induced Electric Discharge Phenomena in Metal–Solvent Mixtures," *ChemistryOpen,* vol. 1, no. 1, pp. 39-48, 2012.

[10] S. Horikoshi, A. Osawa, M. Abe, and N. Serpone, "On the generation of hot-spots by microwave electric and magnetic fields and their impact on a microwave-assisted

heterogeneous reaction in the presence of metallic Pd nanoparticles on an activated carbon support," *The Journal of Physical Chemistry C,* vol. 115, no. 46, pp. 23030-23035, 2011.

[11] S. Horikoshi *et al.*, "Organic syntheses by microwave selective heating of novel metal/CMC catalysts–The Suzuki–Miyaura coupling reaction in toluene and the dehydrogenation of tetralin in solvent-free media," *Journal of catalysis,* vol. 289, pp. 266-271, 2012.

[12] S. Horikoshi, A. Osawa, S. Sakamoto, and N. Serpone, "Control of microwave-generated hot spots. Part IV. Control of hot spots on a heterogeneous microwave-absorber catalyst surface by a hybrid internal/external heating method," *Chemical Engineering and Processing: Process Intensification,* vol. 69, pp. 52-56, 2013.

[13] X. Zhang, D. O. Hayward, and D. M. P. Mingos, "Apparent equilibrium shifts and hot-spot formation for catalytic reactions induced by microwave dielectric heating," *Chemical Communications,* no. 11, pp. 975-976, 1999.

[14] S. Horikoshi, M. Kamata, T. Mitani, and N. Serpone, "Control of microwave-generated hot spots. 6. Generation of hot spots in dispersed catalyst particulates and factors that affect catalyzed organic syntheses in heterogeneous media," *Industrial & Engineering Chemistry Research,* vol. 53, no. 39, pp. 14941-14947, 2014.

[15] Y. Suttisawat, S. Horikoshi, H. Sakai, and M. Abe, "Hydrogen production from tetralin over microwave-accelerated Pt-supported activated carbon," *International journal of hydrogen energy,* vol. 35, no. 12, pp. 6179-6183, 2010.

[16] Y. Suttisawat, S. Horikoshi, H. Sakai, P. Rangsunvigit, and M. Abe, "Enhanced conversion of tetralin dehydrogenation under microwave heating: Effects of temperature variation," *Fuel processing technology,* vol. 95, pp. 27-32, 2012.

[17] S. Horikoshi, M. Kamata, T. Sumi, and N. Serpone, "Selective heating of Pd/AC catalyst in heterogeneous systems for the microwave-assisted continuous hydrogen evolution from organic hydrides: Temperature distribution in the fixed-bed reactor," *International Journal of Hydrogen Energy,* vol. 41, no. 28, pp. 12029-12037, 2016.

[18] R. Manno, V. Sebastian, R. Mallada, and J. s. Santamaria, "110th Anniversary: Nucleation of Ag Nanoparticles in Helical Microfluidic Reactor. Comparison between Microwave and Conventional Heating," *Industrial & Engineering Chemistry Research,* vol. 58, no. 28, pp. 12702-12711, 2019.

[19] A. Ramirez, J. L. Hueso, M. Abian, M. U. Alzueta, R. Mallada, and J. Santamaria, "Escaping undesired gas-phase chemistry: Microwave-driven selectivity enhancement in heterogeneous catalytic reactors," *Science advances,* vol. 5, no. 3, p. eaau9000, 2019.

[20] A. Ramírez, J. L. Hueso, R. Mallada, and J. Santamaría, "Ethylene epoxidation in microwave heated structured reactors," *Catalysis Today,* vol. 273, pp. 99-105, 2016.

[21] A. Ramirez, J. L. Hueso, R. Mallada, and J. Santamaria, "In situ temperature measurements in microwave-heated gas-solid catalytic systems. Detection of hot spots and solid-fluid temperature gradients in the ethylene epoxidation reaction," *Chemical Engineering Journal,* vol. 316, pp. 50-60, 2017.

[22] A. Ramirez, J. L. Hueso, R. Mallada, and J. Santamaria, "Microwave-activated structured reactors to maximize propylene selectivity in the oxidative dehydrogenation of propane," *Chemical Engineering Journal,* p. 124746, 2020.

[23] Y. Suttisawat, H. Sakai, M. Abe, P. Rangsunvigit, and S. Horikoshi, "Microwave effect in the dehydrogenation of tetralin and decalin with a fixed-bed reactor," *International journal of hydrogen energy,* vol. 37, no. 4, pp. 3242-3250, 2012.

[24] N. Haneishi *et al.*, "Enhancement of Fixed-bed Flow Reactions under Microwave Irradiation by Local Heating at the Vicinal Contact Points of Catalyst Particles," *Scientific reports,* vol. 9, no. 1, pp. 1-12, 2019.

[25] T. Durka, G. D. Stefanidis, T. Van Gerven, and A. I. Stankiewicz, "Microwave-activated methanol steam reforming for hydrogen production," *International Journal of Hydrogen Energy,* vol. 36, no. 20, pp. 12843-12852, 2011.

[26] B. T. Ergan, M. Bayramoğlu, and S. Özcan, "Emulsion polymerization of styrene under continuous microwave irradiation," *European Polymer Journal,* vol. 69, pp. 374-384, 2015.

[27] L. Ricciardi, W. Verboom, J. P. Lange, and J. Huskens, "Reactive Extraction Enhanced by Synergic Microwave Heating: Furfural Yield Boost in Biphasic Systems," *ChemSusChem,* vol. 13, no. 14, p. 3589, 2020.

[28] F. Motasemi and A. G. Gerber, "Multicomponent conjugate heat and mass transfer in biomass materials during microwave pyrolysis for biofuel production," *Fuel,* vol. 211, pp. 649-660, 2018.

[29] A. F. Aguilera *et al.*, "Kinetic modelling of Prileschajew epoxidation of oleic acid under conventional heating and microwave irradiation," *Chemical Engineering Science,* vol. 199, pp. 426-438, 2019.

[30] A. F. Aguilera, P. Tolvanen, J. Wärnå, S. Leveneur, and T. Salmi, "Kinetics and reactor modelling of fatty acid epoxidation in the presence of heterogeneous catalyst," *Chemical Engineering Journal,* vol. 375, p. 121936, 2019.

[31] W. Xu, J. Zhou, Z. Su, Y. Ou, and Z. You, "Microwave catalytic effect: a new exact reason for microwave-driven heterogeneous gas-phase catalytic reactions," *Catalysis Science & Technology,* vol. 6, no. 3, pp. 698-702, 2016.

[32] X. Bai, B. Robinson, C. Killmer, Y. Wang, L. Li, and J. Hu, "Microwave catalytic reactor for upgrading stranded shale gas to aromatics," *Fuel,* vol. 243, pp. 485-492, 2019.

[33] J. Hunt, A. Ferrari, A. Lita, M. Crosswhite, B. Ashley, and A. E. Stiegman, "Microwave-specific enhancement of the carbon–carbon dioxide (Boudouard) reaction," *The Journal of Physical Chemistry C,* vol. 117, no. 51, pp. 26871-26880, 2013.

[34] B. Gutmann, A. M. Schwan, B. Reichart, C. Gspan, F. Hofer, and C. O. Kappe, "Activation and deactivation of a chemical transformation by an electromagnetic field: evidence for specific microwave effects in the formation of Grignard reagents," *Angewandte Chemie International Edition,* vol. 50, no. 33, pp. 7636-7640, 2011.

[35] C. O. Kappe, B. Pieber, and D. Dallinger, "Microwave effects in organic synthesis: myth or reality?," *Angewandte Chemie International Edition,* vol. 52, no. 4, pp. 1088-1094, 2013.

[36] S. Hayden, A. F. H. Studentschnig, S. Schober, and C. O. Kappe, "A critical investigation on the occurrence of microwave effects in emulsion polymerizations," *Macromolecular Chemistry and Physics,* vol. 215, no. 23, pp. 2318-2326, 2014.

[37] C. O. Kappe, "Unraveling the mysteries of microwave chemistry using silicon carbide reactor technology," *Accounts of chemical research,* vol. 46, no. 7, pp. 1579-1587, 2013.

[38] J. Robinson *et al.*, "Understanding microwave heating effects in single mode type cavities—theory and experiment," *Physical Chemistry Chemical Physics,* vol. 12, no. 18, pp. 4750-4758, 2010.

[39] B. Ashley, D. D. Lovingood, Y.-C. Chiu, H. Gao, J. Owens, and G. F. Strouse, "Specific effects in microwave chemistry explored through reactor vessel design, theory, and spectroscopy," *Physical Chemistry Chemical Physics,* vol. 17, no. 41, pp. 27317-27327, 2015.

[40] H. Goyal, A. Mehdad, R. F. Lobo, G. D. Stefanidis, and D. G. Vlachos, "Scaleup of a Single-Mode Microwave Reactor," *Industrial & Engineering Chemistry Research,* vol. 59, no. 6, pp. 2516-2523, 2019.

[41] G. S. J. Sturm, M. D. Verweij, T. Van Gerven, A. I. Stankiewicz, and G. D. Stefanidis, "On the effect of resonant microwave fields on temperature distribution in time and space," *International Journal of Heat and Mass Transfer,* vol. 55, no. 13-14, pp. 3800-3811, 2012.

[42] T.-Y. Chen, M. Baker-Fales, and D. G. Vlachos, "Operation and Optimization of Microwave-Heated Continuous-Flow Microfluidics," *Industrial & Engineering Chemistry Research,* vol. 59, no. 22, pp. 10418-10427, 2020.

[43] A. Malhotra *et al.*, "Temperature Homogeneity under Selective and Localized Microwave Heating in Structured Flow Reactors," *Industrial & Engineering Chemistry Research,* vol. 60, no. 18, pp. 6835-6847, 2021.

[44] J. Robinson *et al.*, "Electromagnetic simulations of microwave heating experiments using reaction vessels made out of silicon carbide," *Physical Chemistry Chemical Physics,* vol. 12, no. 36, pp. 10793-10800, 2010.

[45] L. M. Sanz-Moral *et al.*, "Release of hydrogen from nanoconfined hydrides by application of microwaves," *Journal of Power Sources,* vol. 353, pp. 131-137, 2017.

[46] H. Nigar *et al.*, "Numerical analysis of microwave heating cavity: Combining electromagnetic energy, heat transfer and fluid dynamics for a NaY zeolite fixed-bed," *Applied Thermal Engineering,* vol. 155, pp. 226-238, 2019.

[47] G. D. Stefanidis, A. N. Munoz, G. S. J. Sturm, and A. Stankiewicz, "A helicopter view of microwave application to chemical processes: reactions, separations, and equipment concepts," *Reviews in Chemical Engineering,* vol. 30, no. 3, pp. 233-259, 2014.

[48] J. D. Moseley and C. O. Kappe, "A critical assessment of the greenness and energy efficiency of microwave-assisted organic synthesis," *Green Chemistry,* vol. 13, no. 4, pp. 794-806, 2011.

[49] P. Priecel and J. A. Lopez-Sanchez, "Advantages and limitations of microwave reactors: from chemical synthesis to the catalytic valorization of biobased chemicals," *ACS Sustainable Chemistry & Engineering,* vol. 7, no. 1, pp. 3-21, 2018.

[50] S. Horikoshi and N. Serpone, "Role of microwaves in heterogeneous catalytic systems," *Catalysis Science & Technology,* vol. 4, no. 5, pp. 1197-1210, 2014.

[51] S. Chandrasekaran, S. Ramanathan, and T. Basak, "Microwave food processing—A review," *Food Research International,* vol. 52, no. 1, pp. 243-261, 2013.

[52] Y. Zhang, C. Ke, W. Fu, Y. Cui, M. A. Rehan, and B. Li, "Simulation of microwave-assisted gasification of biomass: A review," *Renewable Energy,* vol. 154, pp. 488-496, 2020.

[53] C. Ke *et al.*, "Syngas production from microwave-assisted air gasification of biomass: Part 1 model development," *Renewable Energy,* vol. 140, pp. 772-778, 2019.

[54] Y. Zhang *et al.*, "Syngas production from microwave-assisted air gasification of biomass: Part 2 model validation," *Renewable Energy,* vol. 140, pp. 625-632, 2019.

[55] X. Zhang, K. Rajagopalan, H. Lei, R. Ruan, and B. K. Sharma, "An overview of a novel concept in biomass pyrolysis: microwave irradiation," *Sustainable Energy & Fuels,* vol. 1, no. 8, pp. 1664-1699, 2017.

[56] Y.-F. Huang, P.-T. Chiueh, and S.-L. Lo, "A review on microwave pyrolysis of lignocellulosic biomass," *Sustainable Environment Research,* vol. 26, no. 3, pp. 103-109, 2016.

[57] S. C. Motshekga, S. K. Pillai, S. Sinha Ray, K. Jalama, and R. Krause, "Recent trends in the microwave-assisted synthesis of metal oxide nanoparticles supported on carbon nanotubes and their applications," *Journal of Nanomaterials,* vol. 2012, 2012.

[58] N. Makul, P. Rattanadecho, and D. K. Agrawal, "Applications of microwave energy in cement and concrete–a review," *Renewable and Sustainable Energy Reviews,* vol. 37, pp. 715-733, 2014.

[59] H. Li, Z. Zhao, C. Xiouras, G. D. Stefanidis, X. Li, and X. Gao, "Fundamentals and applications of microwave heating to chemicals separation processes," *Renewable and Sustainable Energy Reviews,* vol. 114, p. 109316, 2019.

[60] D. M. Pozar, *Microwave engineering*. John Wiley & Sons, 2009.

[61] G. S. J. Sturm, M. D. Verweij, A. I. Stankiewicz, and G. D. Stefanidis, "Microwaves and microreactors: design challenges and remedies," *Chemical Engineering Journal,* vol. 243, pp. 147-158, 2014.

[62] B. K. Sahoo, S. De, and B. C. Meikap, "Improvement of grinding characteristics of Indian coal by microwave pre-treatment," *Fuel processing technology,* vol. 92, no. 10, pp. 1920-1928, 2011.

[63] S. Horikoshi, R. F. Schiffmann, J. Fukushima, and N. Serpone, *Microwave Chemical and Materials Processing*. Springer, 2018.

[64] J. Sun, W. Wang, and Q. Yue, "Review on microwave-matter interaction fundamentals and efficient microwave-associated heating strategies," *Materials,* vol. 9, no. 4, p. 231, 2016.

[65] S. Mutyala, C. Fairbridge, J. R. J. Paré, J. M. R. Bélanger, S. Ng, and R. Hawkins, "Microwave applications to oil sands and petroleum: A review," *Fuel Processing Technology,* vol. 91, no. 2, pp. 127-135, 2010.

[66] R. R. Mishra and A. K. Sharma, "Microwave–material interaction phenomena: Heating mechanisms, challenges and opportunities in material processing," *Composites Part A: Applied Science and Manufacturing,* vol. 81, pp. 78-97, 2016/02/01/ 2016.

[67] H. Goyal, S. Sadula, and D. G. Vlachos, "Microwave heating of slurries," *Chemical Engineering Journal,* p. 127892, 2020.

[68] W. Chen *et al.*, "Intensified microwave-assisted heterogeneous catalytic reactors for sustainable chemical manufacturing," *Chemical Engineering Journal,* p. 130476, 2021.

[69] H. M. Nguyen, J. Sunarso, C. Li, G. H. Pham, C. Phan, and S. Liu, "Microwave-assisted catalytic methane reforming: A review," *Applied Catalysis A: General,* vol. 599, p. 117620, 2020/06/05/ 2020.

[70] I. Julian *et al.*, "Overcoming Stability Problems in Microwave-Assisted Heterogeneous Catalytic Processes Affected by Catalyst Coking," *Catalysts,* vol. 9, no. 867, pp. 1-14, 2019.

[71] M. Y. Onimisi, J. T. Ikyumbur, S. G. Abdu, and E. C. Hemba, "Frequency and temperature effect on dielectric properties of acetone and dimethylformamide," *Physical Science International Journal,* pp. 1-8, 2016.

[72] T. Yang, Y. H. Zhou, S. Z. Zhu, H. Pan, and Y. B. Huang, "Insight into aluminum sulfate-catalyzed xylan conversion into furfural in a γ-valerolactone/water biphasic solvent under microwave conditions," *ChemSusChem,* vol. 10, no. 20, pp. 4066-4079, 2017.

[73] L. Simeral and R. L. Amey, "Dielectric properties of liquid propylene carbonate," *The Journal of Physical Chemistry,* vol. 74, no. 7, pp. 1443-1446, 1970/04/01 1970.

[74] V. V. e. Butova, M. A. Soldatov, A. A. Guda, K. A. Lomachenko, and C. Lamberti, "Metal-organic frameworks: structure, properties, methods of synthesis and characterization," *Russian Chemical Reviews,* vol. 85, no. 3, p. 280, 2016.

[75] E. Pert *et al.*, "Temperature measurements during microwave processing: the significance of thermocouple effects," *Journal of the American Ceramic Society,* vol. 84, no. 9, pp. 1981-1986, 2001.

[76] H. Will, P. Scholz, and B. Ondruschka, "Heterogeneous gas-phase catalysis under microwave irradiation—a new multi-mode microwave applicator," *Topics in catalysis,* vol. 29, no. 3-4, pp. 175-182, 2004.

[77] D. V. Suriapparao, N. Pradeep, and R. Vinu, "Bio-oil production from Prosopis juliflora via microwave pyrolysis," *Energy & Fuels,* vol. 29, no. 4, pp. 2571-2581, 2015.

[78] B. R. Reddy and R. Vinu, "Microwave assisted pyrolysis of Indian and Indonesian coals and product characterization," *Fuel Processing Technology,* vol. 154, pp. 96-103, 2016.

[79] D. V. Suriapparao and R. Vinu, "Resource recovery from synthetic polymers via microwave pyrolysis using different susceptors," *Journal of analytical and applied pyrolysis,* vol. 113, pp. 701-712, 2015.

[80] L. S. Gangurde, G. S. J. Sturm, T. J. Devadiga, A. I. Stankiewicz, and G. D. Stefanidis, "Complexity and challenges in noncontact high temperature measurements in microwave-assisted catalytic reactors," *Industrial & engineering chemistry research,* vol. 56, no. 45, pp. 13379-13391, 2017.

[81] K. Knoerzer, M. Regier, E. H. Hardy, H. P. Schuchmann, and H. Schubert, "Simultaneous microwave heating and three-dimensional MRI temperature mapping," *Innovative food science & emerging technologies,* vol. 10, no. 4, pp. 537-544, 2009.

[82] C. Zhang, L. Liao, and S. S. Gong, "Recent developments in microwave-assisted polymerization with a focus on ring-opening polymerization," *Green Chemistry,* vol. 9, no. 4, pp. 303-314, 2007.

[83] C. Ebner, T. Bodner, F. Stelzer, and F. Wiesbrock, "One Decade of Microwave-Assisted Polymerizations: Quo vadis?," *Macromolecular rapid communications,* vol. 32, no. 3, pp. 254-288, 2011.

[84] R. Hoogenboom and U. S. Schubert, "Microwave-assisted polymer synthesis: recent developments in a rapidly expanding field of research," *Macromolecular Rapid Communications,* vol. 28, no. 4, pp. 368-386, 2007.

[85] R.-J. van Putten, J. C. van der Waal, E. de Jong, C. B. Rasrendra, H. J. Heeres, and J. G. de Vries, "Hydroxymethylfurfural, A Versatile Platform Chemical Made from Renewable Resources," *Chemical Reviews,* vol. 113, no. 3, pp. 1499-1597, 2013/03/13 2013, doi: 10.1021/cr300182k.

[86] S. Caratzoulas *et al.*, "Challenges of and insights into acid-catalyzed transformations of sugars," *The Journal of Physical Chemistry C,* vol. 118, no. 40, pp. 22815-22833, 2014.

[87] T.-Y. Chen, Z. Cheng, P. Desir, B. Saha, and D. G. Vlachos, "Fast microflow kinetics and acid catalyst deactivation in glucose conversion to 5-hydroxymethylfurfural," *Reaction Chemistry & Engineering,* 10.1039/D0RE00391C 2021, doi: 10.1039/D0RE00391C.

[88] H. Stange, M. Ishaque, N. Niessner, M. Pepers, and A. Greiner, "Microwave-Assisted Free Radical Polymerizations and Copolymerizations of Styrene and Methyl Methacrylate," *Macromolecular rapid communications,* vol. 27, no. 2, pp. 156-161, 2006.

[89] H. M. Jung, Y. Yoo, Y. S. Kim, and J. H. Lee, "Microwave-Irradiated Copolymerization of Styrene and Butyl Acrylate," *Macromolecular Symposia,* vol. 249, no. 1, pp. 521-528, 2007 2007.

[90] Y. Bo, H. Hui, C. Riping, and J. Demin, "Polysiloxane nanoparticles prepared by emulsion polymerization under microwave irradiation," *e-Polymers,* vol. 8, no. 1, 2008.

[91] R. Karnati and W. T. Ford, "Dispersion copolymerization of 2-ethylhexyl methacrylate and vinylbenzyl chloride and functional group conversions in a fluorinated solvent using

microwave heating," *Journal of Polymer Science Part A: Polymer Chemistry,* vol. 46, no. 11, pp. 3813-3819, 2008.

[92] S. W. Breeden *et al.*, "Microwave heating for rapid conversion of sugars and polysaccharides to 5-chloromethyl furfural," *Green Chemistry,* vol. 15, no. 1, pp. 72-75, 2013.

[93] S. Horikoshi, M. Kamata, T. Mitani, and N. Serpone, "Control of microwave-generated hot spots. 6. Generation of hot spots in dispersed catalyst particulates and factors that affect catalyzed organic syntheses in heterogeneous media," *Industrial and Engineering Chemistry Research,* vol. 53, no. 39, pp. 14941-14947, 2014.

[94] J. A. Menéndez *et al.*, "Microwave heating processes involving carbon materials," *Fuel Processing Technology,* vol. 91, no. 1, pp. 1-8, 2010.

[95] B. Robinson, A. Caiola, X. Bai, V. Abdelsayed, D. Shekhawat, and J. Hu, "Catalytic Direct Conversion of Ethane to Value-added Chemicals Under Microwave Irradiation," *Catalysis Today,* 2020.

[96] N. Haneishi, S. Tsubaki, M. M. Maitani, E. Suzuki, S. Fujii, and Y. Wada, "Electromagnetic and heat-transfer simulation of the catalytic dehydrogenation of ethylbenzene under microwave irradiation," *Industrial & Engineering Chemistry Research,* vol. 56, no. 27, pp. 7685-7692, 2017.

[97] T. Durka, T. Van Gerven, and A. Stankiewicz, "Microwaves in heterogeneous gas-phase catalysis: experimental and numerical approaches," *Chemical Engineering & Technology: Industrial Chemistry-Plant Equipment-Process Engineering-Biotechnology,* vol. 32, no. 9, pp. 1301-1312, 2009.

[98] A. Cybulski and J. A. Moulijn, *Structured Catalysts and Reactors*, 2nd ed. Taylor & Francis Group, LLC, 2006.

[99] E. Bianchi, T. Heidig, C. G. Visconti, G. Groppi, H. Freund, and E. Tronconi, "An appraisal of the heat transfer properties of metallic open-cell foams for strongly exo-/endo-thermic catalytic processes in tubular reactors," *Chemical Engineering Journal,* vol. 198-199, pp. 512-528, 2012.

[100] I. Julian *et al.*, "Overcoming Stability Problems in Microwave-Assisted Heterogeneous Catalytic Processes Affected by Catalyst Coking," *Catalysts,* vol. 9, no. 10, 2019, doi: 10.3390/catal9100867.

[101] L. S. Gangurde *et al.*, "Synthesis, characterization, and application of ruthenium-doped SrTiO3 perovskite catalysts for microwave-assisted methane dry reforming," *Chemical Engineering and Processing-Process Intensification,* vol. 127, pp. 178-190, 2018.

[102] H. Zhang, H. Geerlings, J. Lin, and W. S. Chin, "Rapid microwave hydrogen release from MgH2 and other hydrides," *International journal of hydrogen energy,* vol. 36, no. 13, pp. 7580-7586, 2011.

[103] Y. Mao *et al.*, "Rapid degradation of malachite green by CoFe2O4–SiC foam under microwave radiation," *Royal Society open science,* vol. 5, no. 6, p. 180085, 2018.

[104] P. Wrigstedt, J. Keskiväli, and T. Repo, "Microwave-enhanced aqueous biphasic dehydration of carbohydrates to 5-hydroxymethylfurfural," *RSC advances,* vol. 6, no. 23, pp. 18973-18979, 2016.

[105] B. Liu *et al.*, "Microwaves effectively examine the extent and type of coking over acid zeolite catalysts," *Nature communications,* vol. 8, no. 1, pp. 1-7, 2017.

[106] J. Gallagher, "Microwaving coke," *Nature Energy,* vol. 2, no. 10, pp. 766-766, 2017.

[107] I. de Dios García, A. Stankiewicz, and H. Nigar, "Syngas production via microwave-assisted dry reforming of methane," *Catalysis Today,* vol. 362, pp. 72-80, 2021.

[108] I. Julian *et al.*, "From bench scale to pilot plant: A 150x scaled-up configuration of a microwave-driven structured reactor for methane dehydroaromatization," *Catalysis Today,* 2021.

[109] H. E. Toraman, K. Alexopoulos, S. C. Oh, S. Cheng, D. Liu, and D. G. Vlachos, "Ethylene production by direct conversion of methane over isolated single active centers," *Chemical Engineering Journal,* p. 130493, 2021.

[110] T. Krech, R. Krippendorf, B. Jäger, M. Präger, P. Scholz, and B. Ondruschka, "Microwave radiation as a tool for process intensification in exhaust gas treatment," *Chemical Engineering and Processing: Process Intensification,* vol. 71, pp. 31-36, 2013.

[111] R. Weingarten, J. Cho, W. C. Conner Jr, and G. W. Huber, "Kinetics of furfural production by dehydration of xylose in a biphasic reactor with microwave heating," *Green Chemistry,* vol. 12, no. 8, pp. 1423-1429, 2010.

[112] C. Yi, Z. Deng, and Z. Xu, "Monodisperse thermosensitive particles prepared by emulsifier-free emulsion polymerization with microwave irradiation," *Colloid and Polymer Science,* vol. 283, no. 11, pp. 1259-1266, 2005.

[113] COMSOL Multiphysics v. 5.3, ed: COMSOL AB, Stockholm, Sweden.

[114] P. Magnico, "Hydrodynamic and transport properties of packed beds in small tube-to-sphere diameter ratio: pore scale simulation using an Eulerian and a Lagrangian approach," *Chemical engineering science,* vol. 58, no. 22, pp. 5005-5024, 2003.

[115] N. S. Bakhvalov and G. Panasenko, *Homogenisation: averaging processes in periodic media: mathematical problems in the mechanics of composite materials*. Springer Science & Business Media, 2012.

[116] W. Wang, B. Wang, J. Sun, Y. Mao, X. Zhao, and Z. Song, "Numerical simulation of hot-spot effects in microwave heating due to the existence of strong microwave-absorbing media," *Rsc Advances,* vol. 6, no. 58, pp. 52974-52981, 2016.

[117] D. Zare and M. Ranjbaran, "Simulation and validation of microwave-assisted fluidized bed drying of soybeans," *Drying Technology,* vol. 30, no. 3, pp. 236-247, 2012.

[118] B. A. Souraki, A. Andres, and D. Mowla, "Mathematical modeling of microwave-assisted inert medium fluidized bed drying of cylindrical carrot samples," *Chemical Engineering and Processing: Process Intensification,* vol. 48, no. 1, pp. 296-305, 2009.

[119] C. Si, J. Wu, Y. Zhang, G. Liu, and Q. Guo, "Experimental and numerical simulation of drying of lignite in a microwave-assisted fluidized bed," *Fuel,* vol. 242, pp. 149-159, 2019.

[120] S. S. R. Geedipalli, V. Rakesh, and A. K. Datta, "Modeling the heating uniformity contributed by a rotating turntable in microwave ovens," *Journal of Food Engineering,* vol. 82, no. 3, pp. 359-368, 2007.

[121] G. L. Lee, M. C. Law, and V.-C. Lee, "Numerical modelling of liquid heating and boiling phenomena under microwave irradiation using OpenFOAM," *International Journal of Heat and Mass Transfer,* vol. 148, p. 119096, 2020.

[122] S. Das, N. G. Deen, and J. A. M. Kuipers, "Multiscale modeling of fixed-bed reactors with porous (open-cell foam) non-spherical particles: Hydrodynamics," *Chemical Engineering Journal,* vol. 334, pp. 741-759, 2018.

[123] H. Goyal and P. Pepiot, "A compact kinetic model for biomass pyrolysis at gasification conditions," *Energy & Fuels,* vol. 31, no. 11, pp. 12120-12132, 2017.

[124] H. Goyal, O. Desjardins, P. Pepiot, and J. Capecelatro, "A computational study of the effects of multiphase dynamics in catalytic upgrading of biomass pyrolysis vapor," *AIChE Journal,* vol. 64, no. 9, pp. 3341-3353, 2018.

[125] G. R. Kasat, A. R. Khopkar, V. V. Ranade, and A. B. Pandit, "CFD simulation of liquid-phase mixing in solid–liquid stirred reactor," *Chemical Engineering Science,* vol. 63, no. 15, pp. 3877-3885, 2008.

[126] S. R. Deshmukh, A. B. Mhadeshwar, M. I. Lebedeva, and D. G. Vlachos, "From density functional theory to microchemical device homogenization: model prediction of hydrogen production for portable fuel cells," *International Journal for Multiscale Computational Engineering,* vol. 2, no. 2, 2004.

[127] J. E. Rim, P. M. Pinsky, and W. W. van Osdol, "Using the method of homogenization to calculate the effective diffusivity of the stratum corneum," *Journal of Membrane Science,* vol. 293, no. 1-2, pp. 174-182, 2007.

[128] J. L. Auriault and J. Lewandowska, "Homogenization analysis of diffusion and adsorption macrotransport in porous media: macrotransport in the absence of advection," *Geotechnique,* vol. 43, no. 3, pp. 457-469, 1993.

[129] A. Dasgupta and R. K. Agarwal, "Orthotropic thermal conductivity of plain-weave fabric composites using a homogenization technique," *Journal of Composite Materials,* vol. 26, no. 18, pp. 2736-2758, 1992.

[130] Y. Asakuma, S. Miyauchi, T. Yamamoto, H. Aoki, and T. Miura, "Homogenization method for effective thermal conductivity of metal hydride bed," *International Journal of Hydrogen Energy,* vol. 29, no. 2, pp. 209-216, 2004.

[131] H. Goyal and D. G. Vlachos, "Multiscale modeling of microwave-heated multiphase systems," *Chemical Engineering Journal,* p. 125262, 2020.

[132] K. G. Ayappa, H. T. Davis, G. Crapiste, E. A. Davis, and J. Gordon, "Microwave heating: an evaluation of power formulations," *Chemical engineering science,* vol. 46, no. 4, pp. 1005-1016, 1991.